CAVITY SURFACE EMITTING LASERS (VCSELS)

by

SANJAY JAMINDAR

LASER TECHNOLOGY PROGRAMME

RICAL SIMULATION OF TURN-ON JITTER SINGLE-MODE SINGLE-POLARIZATION RTICAL CAVITY SURFACE EMITTING LASERS(VCSELs)

A Thesis Submitted
in Partial Fulfillment of the Requirements
for the Degree of

MASTER OF TECHNOLOGY

by

SANJAY JAMINDAR

to the

LASER TECHNOLOGY PROGRAMME
INDIAN INSTITUTE OF TECHNOLOGY KANPUR

April, 1999

Dedicated to my parents

FACHBEREICH 12
ELEKTROTECHNIK
Fachgebiet
Hochfrequenztechnik
Prof. Dr.-Ing. K. Petermann
Tel.: ++49 / 30 / 23346

Technische Universität Berlin Fachgebiet Hochfrequenztechnik
Sekr. HFT 4-1 Einsteinufer 25 D- 10587 Berlin

Datum: 05.01.99

Certification

for Mr. Sanjay Jamindar

This is to certify that the thesis entitled " ***Numerical Simulation of Turn-On Jitter for Single-Mode Single-Polarization VCSEL***" submitted by Mr. Sanjay Jamindar to the Indian Institute Of Technology, Kanpur, India for the award of the degree of ***Master Of Technology*** (M.Tech) is a bonafide record of research work carried out by him under my supervision at the Technical University Berlin, Germany. The contents of this thesis, in full or in parts, have not been submitted to any other Institute or University for the award of any degree or diploma."

(Prof. Dr.-Ing. Klaus Petermann)

Tel.: (030) 314-23346 • Sekr.: Tel.: (030) 314-22637 • Telefax: (030) 314-24626 • e-mail: petermann@tu-berlin.de

CERTIFICATE

This is to certify that the work contained in the thesis entitled " *Numerical Simulation of Turn-on Jitter of Single-mode Single-polarization Vertical Cavity Surface Emitting Lasers(VCSELs)*" by Mr. Sanjay Jamindar (Roll No: 9711605), has been carried out under the joint supervision of Prof. K. Petermann & Dr. J. John and this work has not been submitted elsewhere for a degree.

Thesis Supervisor.

28 April, 1999

Dr. Joseph John
Associate Professor
Dept. of Electrical Engineering
Indian Institute Of Technology
Kanpur.

ACKNOWLEDGEMENTS

I am very much grateful to Prof. K. Petermann, who provided me an opportunity to work under his supervision at The Institute Of High Frequency Technique(HFT), Technical University, Berlin, Germany. His invaluable suggestions and ideas about the work helped me to complete it in time. He had been a constant source of encouragement.

I would like to express my deep and sincere gratitude to Dr. J. John, Indian Institute Of Technology, Kanpur, for his invaluable ideas, constant supervision and inspiration. I appreciate the extra effort that he had to put in for guiding me through modern means of communication like e-mail since the research work reported in this project was carried out at Technical University, Berlin. He regularly kept in touch with me and discussed about the work through mail.

Next I would like to thank Dip. Ing. Li-Gao Zei for his constant guidance and invaluable help in keeping the project in the right direction. He was always available and he never felt disturbed whenever I wanted help from him. We discussed ourselves a lot about the work.

I would like to express my sincere thanks to Deutscher Akademischer Austauschdienst (DAAD) who provided me a scholarship to pursue my M.Tech thesis in Germany under their new Sandwich Scholarship programme with IITs in India.

I would also like to thank my Indian friends from different IITs who came and stayed with me in nine months in Germany under the same exchange programme. With them I always felt homely in this completely new surroundings and this helped me to complete my project in time.

At last I would like to say that without the inspiration from my parents and sisters I could not have completed the work satisfactorily during my first time abroad. They, especially my elder sister, Mrs. Sangita Chakraborty always gave me inspiration through e-mail so that I could carry on my work smoothly.

Sanjay Jamindar.

Place: Berlin
Date: 20-12-98

(Sanjay Jamindar)

CONTENTS

References

Appendix

Abstract

A simulation model of *Single-mode Single-polarization* Vertical Cavity Surface Emitting Laser (VCSEL) is developed by which the turn-on event of the VCSEL can be simulated by solving the rate equations numerically after introducing the parameters of the VCSEL to be simulated in the laser rate equations. The numerical solution of the coupled rate equations is done by 4^{th} order Runge-Kutta method using the software LabVIEW. The spontaneous emission noise is simulated by using Langevin noise sources in the equations. From the statistical behaviour of the turn-on delay of the zero-biased laser, the *probability density function(PDF)* of the turn-on delay is calculated and plotted for different on-states. The *turn-on jitter* is calculated which is the standard deviation of the PDF. Also the *relaxation resonance frequency* is calculated for different on-states. Then the variation of jitter with relaxation resonance frequency (i.e. the variation of jitter with different on-states) is compared with the analytical expression derived from the theory and also with the measurement results. Also the effects of different off-states on jitter is investigated. Further the effects of different bit patterns and also the effects of bit rates on jitter is investigated.

For the simulation of the VCSEL, the data rate taken for simulation of jitter is 160 Mbits/s. Also the simulation is extended to 1 Gbits/s. First, the 1010 pattern is applied and then the pseudo-random pattern is applied to observe the bit pattern effect.

The laser characteristic graph obtained from simulation is matching well with the experimental graph although the effect of suppressed polarization is neglected in simulation. Also, the variation of jitter with relaxation resonance frequency (f_r) is in good agreement with the measurement results as well as with the theory. When the relaxation resonance frequency exceeds 3 GHz, the variation of jitter with f_r is not matching with the experimental results as the laser is multimode when f_r exceeds 3 GHz as obtained experimentally. Also, it is observed that turn-on jitter does not depend on off-states as long as the off-states is below threshold, but if the off state is above threshold jitter decreases. Additionally, it is found that jitter increases due to bit pattern effect when the data rate is high enough and pseudo-random pattern is applied.

Chapter 1

Introduction

The vertical cavity surface emitting laser (VCSEL) is emerging as the light source of choice for modern high speed, short wavelength communication systems.For short distance links it is of great interest to use Vertical Cavity Surface Emitting Lasers(VCSELs) as light sources[2] In order to simplify the driving circuits as well as to reduce the electrical power consumption, zero(or constant) biased operation is required. It is well known that this kind of operation leads to a significant turn-on jitter due to spontaneous emission and the bit pattern effect. In a digital transmission system an enhancement of the turn-on jitter increases the bit error rate(BER) especially at high data rate, which can affect the performance of the system significantly[2].

1.1 Vertical Cavity Surface Emitting Lasers (VCSELs) : An Introduction

The information below about VCSEL has been reproduced from the journal of Siemens Fiber Optics, Berlin, Germany [1].

Introduction

The difference in the basic structure of a conventional edge emitting type laser and a VCSEL is that for the edge emitting laser the light propagation is in the plane of the wafer whereas it is *perpendicular to the wafer surface in the VCSEL*(Fig.1). A standard length for edge emitting lasers is 300µm whereas the *active length in a VCSEL is typically only 24nm*. This is the length where the lightwave must pick up all energy. *Therefore mirrors with a very high reflectivity exceeding 99% are required in a VCSEL to enable laser operation.*. In edge emitting laser the cleaved facets with a reflectivity of approximately 30% are sufficient to support lasing. Due to the waveguide design the output beam of conventional lasers exhibits an asymmetric shape with a relatively large divergence. In a VCSEL we have a large amount of freedom in the design of the shape of the active area. So we can tailor it to fit best to our application. In particular we can choose a round shape to obtain a *highly symmetric circular output beam with a small divergence angle which eases coupling to optical fibers*

The good news for industrial applications is the *potential low fabrication and packaging cost of a VCSEL*. In fact, this is what drives the enormous interest in this young technology. The reason for low cost is that we can employ *standard IC fabrication technologies to make the devices*. All the fabrication and testing is done on wafer level with no cleaving and expensive handling of laser bars necessary. Since there is no cleaving, VCSEL wafers are not thinned to a fragile membrane like conventional lasers making the handling of these thinned wafers a nightmare for any production line.

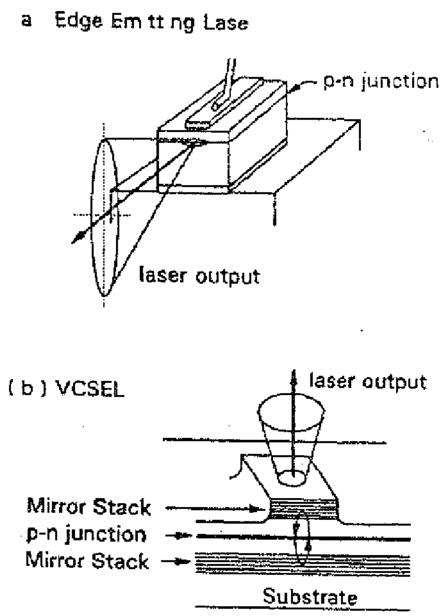

Fig1 Basic difference between Edge-Emitting Laser and VCSEL

History[1]

The idea to built a semiconductor laser diode with a vertically oriented optical resonator was originally developed by Professor Kenichi Iga from the Tokyo Institute of Technology in Japan in the late 70's. In these lasers the light propagates perpendicular to the wafer surface within a very short cavity. The mirrors for optical feedback are made of dielectric multilayer stacks on either side of the epitaxially grown semiconductor active layer. After five years research Professor Iga's group was able to demonstrate the first pulsed operating VCSEL at room temperature in 1984. Four years later continuous wave operation at room temperature was achieved with threshold currents of 32mA.

The major breakthrough in VCSEL technology happened one year later when Jack Jewell from AT & T bell Labs, New Jersey, USA, and Axel Scherer and Jim Harbinson from Bellcore, New Jersey, USA, together with some coworker could demonstrate the first all-epitaxially grown VCSEL on a GaAs substrate. Many hundred extremely thin semiconducto layers built the highly reflecting mirrors of this device. One quantum well with a thickness o just 20 atomic layers provided all the optical amplification of the travelling lightwave. These micro-cavity laser diodes showed sensationally low threshold currents of 1.5 mA.

These results initiated a boom in VCSEL research activities worldwide. Attracted by the remarkable research results companies began to show interest. Today there are eight companies and several research institutes in the U.S. with VCSEL activities. Some compani are manufacturing VCSEL already. The rest of the world follows at some slower speed but i starting to turn the sails in the wind.

design[1]

design must provide an optical confinement for the lightwave prop
electrical confinement for the current which drives the laser. This i
her laser. Among the various approaches to achieve these two main
mostly favoured in fig2. *The light in the VCSEL bounces up and d*
ighly reflecting semiconductor multilayer stacks on either side of th
eedback from the mirrors leads to an optical intensity within the la
orders of magnitude stronger than the electrical field intensity of t
The light emission is mostly through the top mirror. Bottom emissi
nsparent substrate. This is the case for 980 nm VCSELs.

r type VCSEL the fabrication process is non-planar with etch depth
laser current flows from a contact metallization on top of the etche
of the top mirror into the active layer and then spreads out in the b
As substrate. The mesa structure provides an optical waveguide for
centrates the current in a finite area of the active layer. Etching is
ove the active layer to ensure reliable device operation. Motorola e
L.

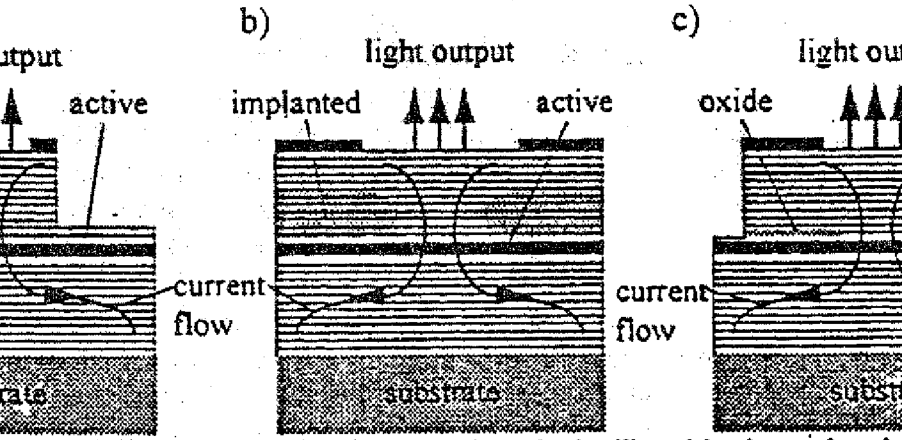

atics of three types of VCSELs: a) etched pillar, b) planar ion im
th AlAs oxidation.

VCSEL provides a planar fabrication process. Deeply implanted pr
istive layers buried in the top mirror which funnels the laser curren
nplantation damage can affect the reliability of the laser. The optica
e implanted semiconductor regions limits the efficiency of these las
% for the best devices reported in the literature. Proton implanted V
oneywell and a lot of other companies due to their relatively easy fa

type employs the *selective oxidation* of a very thin AlAs layer in th
highly resistive layer of AlO_x just above the active layer. This oxide
laser current and builds an optical waveguide at the same time. Th
n these devices *resulting in record performance data of efficiency(*

and extremely low threshold currents (<100μA). The strain from the oxide layer might affect the reliability of these lasers, but first life time test show very promising results. Siemens is looking at this advanced type of VCSEL.

VCSEL performance[1]

VCSELs exhibit excellent performance compared with other lasers. VCSEL threshold currents of less than 100μA have been reported. These numbers are lower than for any other semiconductor laser diode. Reported efficiencies of >50% for VCSELs are difficult to achieve with edge emitting lasers, especially in the low operating current regime. The differential resistance is typically higher for VCSELs than for edge emitters due to the smaller active area but numbers of 50ohm or even less have been demonstrated.

Up today the highest reported output power of a large area VCSEL is around 200 mW for CW operation. The maximum output power is limited by thermal roll-over. It can be increased in the future by improved heat sinking. Large two dimensional VCSEL arrays could generate huge optical output power levels by simply up-scaling the total lasing area. Therefore the devices are also attractive for high power applications.

A unique feature of properly designed VCSELs is the flat temperature response of the threshold current. Fig 3 shows the measured threshold current of a VCSEL in the temperature range between 24°C and 80°C. The threshold current exhibits only a slight variation with a minimum of approximately 550μA at a temperature of about 60°C. We note that the concept of the empirical parameter T_o to describe the high temperature performance of conventional lasers fails in the case of VCSELs. There is no parameter like T_o for VCSELs.

The unusual decrease of threshold current with temperature is caused by the relative wavelength shift of the lasing mode towards the spectral maximum of the optical gain of the active material. Therefore the modal gain for a certain current can be larger at a higher temperature. Thus less current is required to reach the lasing threshold. Since the short cavity of the VCSEL enables only one longitudinal modes there is no mode hopping with increasing temperature like there is in edge emitting lasers.

The optical output power of the VCSEL can be almost constant over a wide temperature range, because the lower threshold current compensates the decreasing efficiency of the device. Fig 3 depicts the measured output power of a VCSEL at a constant drive current over the ambient temperature range between 24°C and 80°C. We note that neither optical feedback nor a monitoring photodiode is necessary for the VCSEL if the system application allows some output power variation. Thus the design of the whole system can be much simpler.

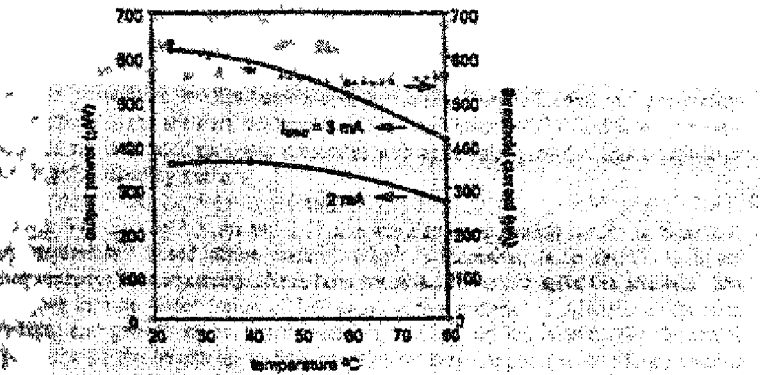

...old current and output power at constant drive current of a VCSEL (Siemens) as ...mbient temperature.

...wavelength[1]

...VCSEL work so far has been done on devices with an emission wavelength of ...n for data communication application. Table 1 gives an overview of the differe... ...ed or discussed for VCSELs from the visible blue/green to the long wavelengt... telecom applications.

...aterial, performance and difficulties for VCSELs in the different waveleng... ...m visible blue/green to long wavelength infrared.[1]

visible blue	*visible green*	*visible red*	*IR* (780-1000nm)	LW (1.3-1.55μm)
InGaN	InGaN	InAlGaP	GaAs, InGaAs	InGaAsP
GaN/AlGaN	GaN/AlGaN	AlGaAs/AlAs	AlGaAs/AlAs	dielectric, wafer fused GaAs/AlAs, InGaAsP/InP
sapphire, SiC	sapphire, SiC	GaAs	GaAs	InP, GaAs
not done	not done	good	excellent	satisfactory research
growth	growth	high temp. performance	no major	mirror technology, high temp.performance

...the wavelength range between 780nm and 980nm are based on GaAs or InGa... ...lls and are relatively easy to fabricate. They exhibit excellent performance and ...n at various places already. Visible VCSELs with an emission wavelength of ...n have been made using InAlGaP active quantum wells. They will come into ...oon. The main application are data storage, plastic optical fibers and laser

pointers. All these VCSELs are fabricated on GaAs substrates with epitaxially grown AlGaAs multilayer stacks to form highly reflecting mirrors.

Long wavelength VCSELs at 1.3 µm and 1.55 µm wavelength are much harder to fabricate, because they require InP based active material which is incompatible to the GaAs based semiconductor mirrors. Several attempts have been made worldwide to solve the problem. The applied techniques include wafer fusion of InP based active material to AlAs/GaAs mirrors, dielectric mirrors and growth of Sb based materials, but we are still waiting for the major breakthrough. None of the results up to now seem to be easily applicable to a large volume production of reliable VCSELs.

The situation in the visible blue/green spectrum is basically a material growth problem of GaN based compounds. GaN/AlGaN multilayer stacks would enable highly reflecting mirrors for VCSELs in this wavelength regime. Since there have been recent reports on GaN based inplane laser from Nichia and Toshiba we can be optimistic to see a GaN based VCSEL in the near future.

Comparison with other light sources[1]

It is interesting to compare features of VCSELs with other light sources used in optoelectronics. Table 2 summarises some important features.

Table 2: Comparison of LEDs, VCSELs, and edge emitting lasers with typical numbers[1]

Property	LED(Surface Emitting)	VCSEL	Edge Emitting Laser
Beam shape	circular	circular	elliptical,astigmatic
Beam divergence	160 degree	13 degree	20 deg.* 60 deg.
Power consumed	100mW	20 mW	100mW
Power emitted	0.1mW	2 mW	30mW
Spectral width	100's A	1e-3A	1e-3A
Spectral temp. dependence	3 A/deg. C	0.6 A/deg.C	3 A/deg. C
Mode hopping	not applicable	no	yes
Output temp.dependence	monotonic moderate degradation	stable for 50deg.-100degC	monotonic degradation
Distance of active region from chip edge	100's µm	100's µm	0 µm
Device uniformity	high	high	low
Testing	on wafer	on wafer	component only
Packaging	straightforward	straightforward	complex
Arrays	1D and 2D	1D and 2D	1D only
Speed	low, 100Mbits/s	high, Gbits/s	high, Gbits/s
Tatal cost	low	low	high

From Table 2 we see that VCSELs combine the best of LEDs and laser diodes They are as cheap and as easy to handle and to package as LEDs but they provide the speed and the high output power of a laser diode. In fact it is HP's philosophy to treat VCSELs simply as fast LEDs. It is obvious that such a device is very attractive for many application.

Advantages of VCSELs

Performance issues

- Surface-Normal output
- Ultra-low lasing threshold
- Dynamic single-mode operation
- Circular, low divergence astigmatic-free beam
- Extremely high electrical to optical power conversion efficiency
- Thermally stable operation
- High speed
- Extremely small active volumes
- 1- and 2-D arrays

Systems issues

- Efficient coupling to fibers
- Insensitivity to feedback
- Densely packed two-dimensional arrays
- Long lifetime
- Compatibility with electronics

Manufacturing issues

- Low cost wafer-scale chip production
- On-wafer testing and screening
- Simplified mounting and packaging

ns

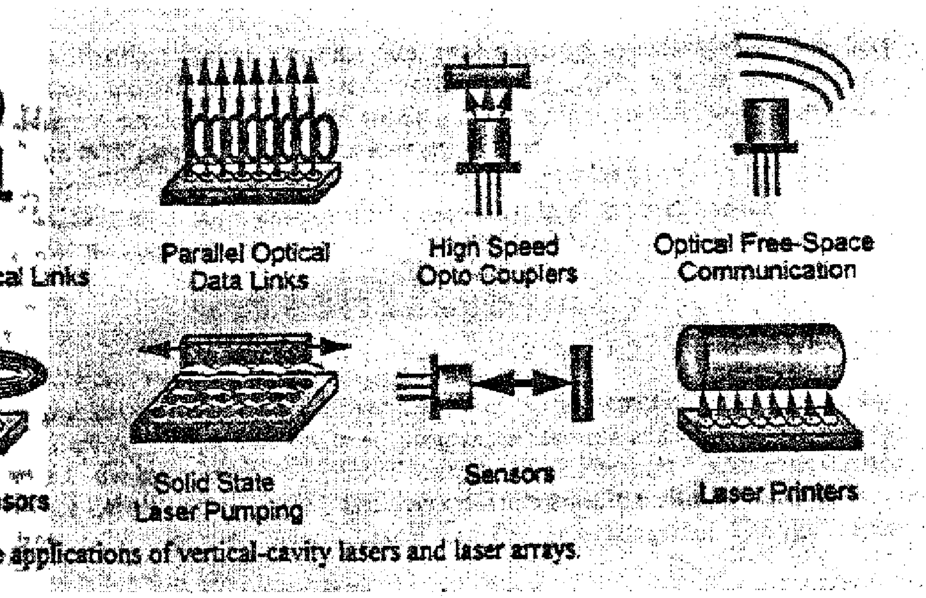

applications of vertical-cavity lasers and laser arrays.

few examples of the application for VCSELs. In serial optical links VCSELs
, due to the higher speed. Gigabit Ethernet is one example for this kind of system
are used in parallel optical data links aim at the server, supercomputer, and
ch market where very high data rates have to be transmitted over distances up to
gher speed of VCSELs compared to LEDs is also attractive for high speed opto
bit rate of more than 10Mbits/s. The volume for opto couplers is high compared
m market, but the price per VCSEL must be very low in order to compete on the
cal free space communication systems work very much like a TV remote control.
rovides data transfer for example from a PC to a printer through air by IR
ead of using a cable.
are a huge market for VCSELs. In the traditional way of a CD player the
s encoded optically on the disk and the laser beam reads the information.

high power capability and high efficiency of VCSEL arrays is attractive for
d state lasers. Furthermore it is a lot easier to attach a VCSEL than an edge
r to the solid state laser. This reduces the cost of the whole system dramatically
arket is full of different application. Large market volumes are predicted for
ing in automotive applications and encoders to find the exact position of rotating
parts. Also laser printers which mostly LEDs today are a possible market for
arrays.
ications VCSELs are just a replacement for conventional lasers or LEDs like in
ks where VCSELs are the better choice due to lower cost and/or higher
Other application require some of the unique features of VCSELs and it is very
e job done with conventional lasers. This is true for most applications which
arrays like disk sensors, high power pump sources, and laser printers.

Conclusion

VCSELs are very attractive for the optoelectronics industry due to their specific feature

1. Potentially low fabrication and packaging cost (non hermetically sealed packages).
2. VCSELs are attractive sources for low-cost, high speed and high-performance, manufacturable parallel optical interconnect modules.
3. Standard IC fabrication processes on full wafers (no cleaving, no handling of small pieces).
4. Wafer scale testing.
5. Single mode emission.
6. Circular output beam shape with low divergence.
7. No HR/AR facet coating.
8. Easy fiber coupling, no additional lenses necessary.
9. Easy integration with other optical elements.
10. VCSELs can also be fabricated with different emission wavelengths within a 2D array in a controllable fashion. Thus, wavelength division multiplexing (WDM) applications are feasible.

Surface Emitting Laser

Introduction

It is well known that biasing a laser near or below threshold can significantly increase the bit-error rate (BER) of optical communication links operating at gigabits rates[2]. However, there are application such as optical interconnects, where zero biased modulation is preferred since it eliminates the need for optical monitoring and feedback control of the bias point. It is of great interest to operate VCSELs in optical interconnects with zero bias since the laser driving circuit is simplified and power consumption can be reduced[2].

Considering the corresponding turn-on event, the BER degradation due to an improper biasing can be easily understood. When a laser is suddenly switched from below to above threshold, the optical emission will be randomly delayed. *The turn-on delay is defined as the time for the photon population to grow from its initial value at the moment of excitation to the stationary value of the on state[2].* Due to spontaneous emission during turn-on there is random fluctuation of turn-on delay. *The **turn-on jitter** is defined as the standard deviation of the probability density function (PDF) of this turn-on delay[2].* There are two main mechanisms which contributes to the turn-on jitter: spontaneous emission and bit-pattern effect. *Due to this turn-on jitter there is significant BER at gigabit data rates. Although at low data rates the BER is not significant due to this jitter[2].*

Theory

An analytical expression to describe the probability density function (PDF) for the turn-on delay for a single-mode edge emitting laser was given in [2]. In contrast to the single TE-polarization state in edge emitting lasers usually two orthogonal polarizations contribute to the emitted light of single mode VCSELs. The PDF for the turn-on delay of a transversal single mode VCSEL with two orthogonal polarizations can be derived in a similar way as shown in [3].

Let us consider a turn-on event as sketched in Fig.2.2.1. The laser drive current is switched on at t=0 from its bias value $I_{off} < I_{th}$ to $I_{on} > I_{th}$ with I_{th} denoting the threshold current. The photon number S within the cavity will then increase starting from the initial value S(0). In order to calculate the statistical properties of the turn-on delay t_d a model has been used here(e.g., [2], [3]) which splits the behaviour of the laser into a stochastic and a deterministic regime similar to that originally proposed in [3]. In contrast to this approach, it has been assumed here that for every turn-on event (i.e., for every combination I_{off}, I_{on}) there is a certain t_c which separates the two regimes. For $t <= t_c$ the photon number is very small and fluctuates strongly due to the dominance of the spontaneous emission.. This leads to an exponential PDF of the photon population which can be assumed is still valid at the crossing time t_c according to

$$p\ S) \quad (1/\ S_c\ )\exp(\ \ S\ /\ S \qquad (2\ 2\ 1)$$

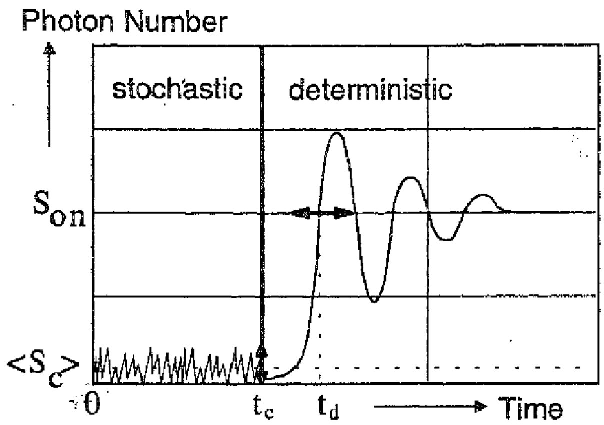

Fig. 2.2.1

where, S_c, $\langle S_c \rangle$ denotes the photon number and its average at $t=t_c$, respectively. $\langle S_c \rangle$ corresponds to the „absorbing barrier" as introduced in [4], [5]. In contrast to the crossing time t_c, the value of $\langle S_c \rangle$ is independent of the specific turn-on event. For $t>t_c$, the laser enters the deterministic region, where the additional time $t_{on} = t_d - t_c$ for the photon population to grow from S_c to the stationary value at the on-state S_{on} is given as [6]

$$\mathbf{t_{on} = (1/2\pi f_r)\sqrt{2\ln(S_{on}/S_c)}} \quad ...(2.2.2)$$

with f_r denoting the relaxation resonance frequency.

Since VCSELs have two polarizations, the PDF of the photon number in each polarization i=1,2 of the SM VCSEL is given by

$$p(S_{c,i}) = (1/\langle S_{c,i} \rangle)\exp(-S_{c,i}/\langle S_{c,i} \rangle), \qquad i=1,2 \quad ...(2.2.3)$$

At the crossing time t_c, $S_{c,i}$ and $\langle S_{c,i} \rangle$ denote the photon number and its mean value in the considered polarizations.

In the case of the SM-VCSEL both polarizations contribute to the total photon number $S_c = S_{c,1} + S_{c,2}$ and its mean value $\langle S_c \rangle = \langle S_{c,1} \rangle + \langle S_{c,2} \rangle$.

The PDF of S_c is given by the convolution of the PDFs of both polarizations yielding

$$p(S_c) = (4S_c/\langle S_c \rangle^2) \cdot \exp(-2S_c/\langle S_c \rangle) \quad ...(2.2.4)$$

where $\langle S_{c,1} \rangle = \langle S_{c,2} \rangle = \langle S_c \rangle / 2$ is assumed.
In the deterministic region t_{on} is given by eqn. (2.2.2) for a known S_c.

The PDF for the photon number S_c can be transformed into a PDF for the turn-on delay using the relation $p(t_{on})dt = p(S_c)dS_c$ yielding

$$\mathbf{p(t_{on}) = 4\omega_r^{\,2} t_{on} (S_{on}^{\,2} / \langle S_c \rangle^2) \cdot \exp[-(\omega_r t_{on})^2] \cdot \exp[-2S_{on} / \langle S_c \rangle \exp[-(\omega_r t_{on})^2/2]]} \quad \text{...(2.2.5)}$$

where $\omega_r = 2\pi f_r$.

The turn-on jitter is given by the standard deviation of eqn. (2.2.5).

Once we have determined the value of the " absorbing barrier" $\langle S_c \rangle$ (which varies from one laser to other), the probability distribution according to (2.2.5)*is only dependent on* f_r and S_{on}. It turns out that $p(t_{on})$ depends weakly on the photon ratio $S_{on}/\langle S_c \rangle$ compared to the dependence on f_r. Furthermore, since f_r *is proportional to* $\sqrt{S_{on}}$, the relaxation resonance frequency can be considered as the main relevant parameter.

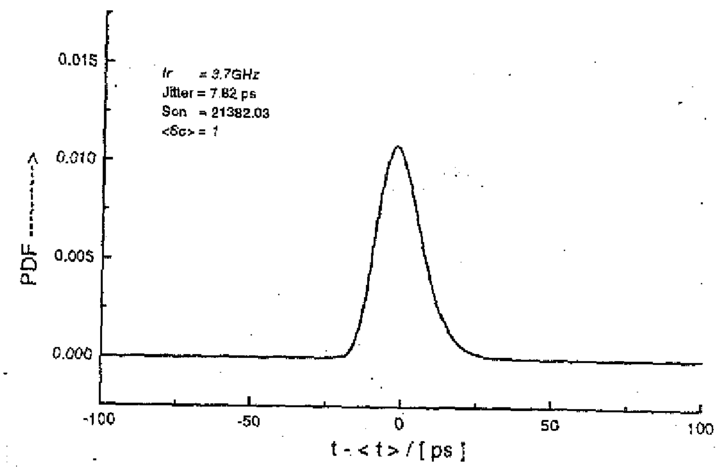

Fig. 2.2.2

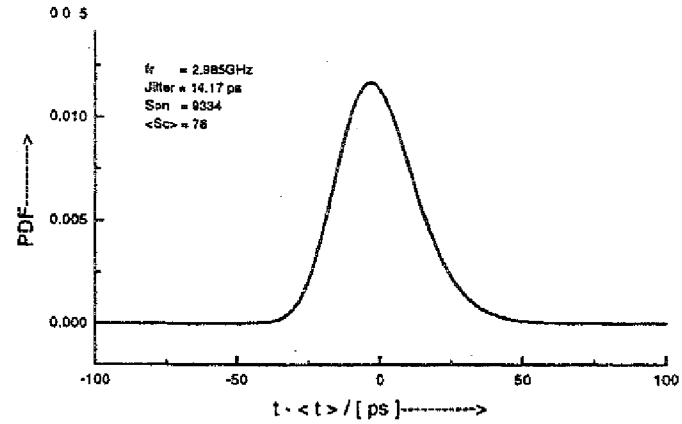

Fig. 2.2.3

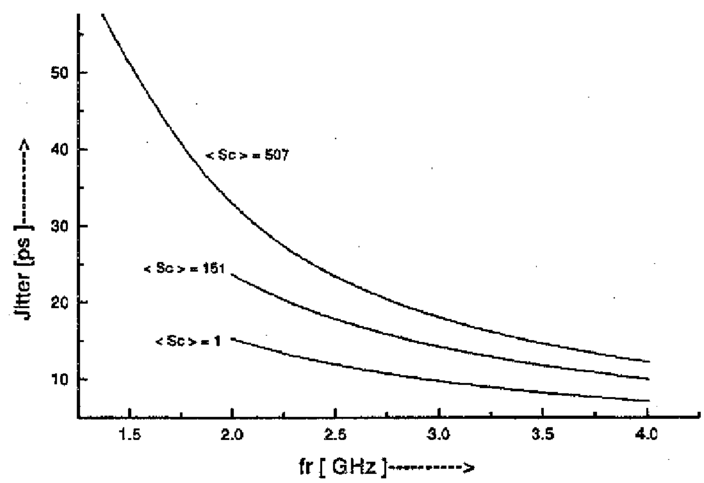

Fig. 2.2.4

Fig. (2.2.2) and (2.2.3) shows the PDF of the turn-on delay for f_r =3.7 GHz and f_r =2.985 GHz respectively with different $\langle S_c \rangle$ s using the eqn. (2.2.5). The turn-on jitter for different $\langle S_c \rangle$ s versus relaxation resonance frequency f_r is plotted in fig. (2.2.4) using the eqn. (2.2.5). So, according to the theoretical model above, for a particular VCSEL(i.e for a given $\langle S_c \rangle$) the jitter decreases with the increase of f_r i.e, with the increase of on-state level.

1 3 General Normalized Rate Equations

Starting from the basic rate equations the normalized rate equations has been derived here which is suitable for solving it numerically [7].

We have the basic rate equation for photons as

$$\mathrm{d}S/\mathrm{d}t = S(R_{st} - 1/t_{ph}) + R_{sp} \quad ...(2.3.0)$$

Where spontaneous emission coefficient $R_{sp} = \Gamma r_{sp}$ and stimulated emission coefficient $R_{st} =$ Γr_{st} and S is the photon numbers.
r_{sp} = Spontaneous emission rate.
r_{st} = Stimulated emission rate.
Γ = Confinement factor.
t_{ph} = Photon life time .

In the rate equation above the term SR_{st} defines the number of photons generated per unit time due to stimulated emission while the term S/t_{ph} defines the number of photons lost per unit time due to recombination. The term R_{sp} defines the spontaneous generation of photons.

For laser operation we can introduce a factor called inversion factor n_{sp} . Under typical lasing condition $n_{sp} = 2.5$

After introducing n_{sp} we can write

$$R_{sp} = n_{sp}\, R_{st} \approx n_{sp} / t_{ph} \quad ...(2.3.1)$$

The expression in eqn. (2.3.1) is valid for $I > I_{th}$.Thus we can neglect the photon number produced by spontaneous emission and we get for stimulated emission $R_{st}(n = n_{th}) \approx 1/t_{ph}$

Now we have the rate equation for electrons as :

$$\mathrm{d}n/\mathrm{d}t = (I/e) - R(n) - R_{st}S \quad ...(2.3.2)$$

where, the spontaneous recombination rate is represented by $R(n)$, the injection current by I and e is the elementary charge. SR_{st} defines the carrier consumption due to stimulated emission.
For the recombination rate $R(n)$ we can assume $R(n) = n / t_e$, where n is the carrier number in the laser cavity and t_e is the carrier life time in the active region.

Now for a particular photon energy gain depends on the carrier density as

$$g_{st}(n) = (a/V)(n - n_0) \quad ...(2.3.3)$$

Where $g_{st}(n)$ is the stimulated gain at the carrier density n/V and n_0/V is the carrier density at population inversion, a is some constant and V is the volume of the active region.

Taking the confinement factor into account we can write effective gain $g = \Gamma g_{st}$.

Now, since stimulated gain coefficient $g_{st} = r_{st}/v_{gr}$, $\therefore g = R_{st}/v_{gr}$
Where, v_{gr} is the group velocity of the optical wave in the active region.

So, the threshold gain g_{th} is given by

$$g(n_{th}) = R_{st}(n_{th})/v_{gr} = 1/t_{ph}v_{gr} = g_{th} \quad ...(2.3.4)$$

So, we can write normalised gain $G = g/g_{th} = R_{st}t_{ph}$ ...(2.3.5)
Since, $n \approx n_{th}$ above threshold, we have $g \approx g_{th}$ i.e, $G \approx 1$ for lasing operation.

Now, the condition for stationary laser operation is

$$\sqrt{R_1 R_2}\exp((g - \alpha_s)L) = 1 \quad ...(2.3.6)$$

where, α_s is scattering loss in the cavity per unit length, L is the length of the cavity and R_1, R_2 are the reflectivities of the two mirrors.

Therefore we can write

$$g_{th} = \alpha_s + (1/2L)\ln(1/R_1R_2) \quad ...(2.3.7)$$

Now, n_{th} is the threshold carrier number, where the loss in the cavity is compensated by the stimulated emission and is given by

$$n_{th} = n_0 + (1/(t_{ph}v_{gr}\Gamma(a/V))) \quad ...(2.3.8)$$

By introducing the normalized gain $G = g/g_{th} = R_{st}\,t_{ph}$ we can write the rate equations (2.3.0) and (2.3.2) as follows

$$\mathbf{dn/dt = I/e - R(n) - GS/t_{ph}} \quad ...(2.3.9)$$
$$\mathbf{dS/dt = (S/t_{ph})(G-1) + K_{tot}R_{sp}} \quad ...(2.3.10)$$

where K_{to} is the enhancement factor for spontaneous emission.

In order to account for the nonlinear gain the gain G can be splitted into linear and nonlinear part as

$$G = G_l(1-\kappa_p P) = G_l(1-\kappa_s S) \quad ...(2.3.11)$$

where G_l is the linear gain and
κ_p is the gain compression coefficient related to optical power and
κ_s is the gain compression coefficient related to photon numbers.
The relation between κ_s and κ_p is given by

$$\kappa_s = (1/2)\, h\nu v_{gr} \cdot (\ln(1/R_1R_2)) \cdot \kappa_p/(2L) \quad ...(2.3.12)$$

where $h =$ Planck's constant
$\nu =$ Freq. of the emitted light

In order to solve the above differential equations numerically it is necessary to normalized the equations as

$$\begin{aligned} \mathbf{S_N} &= \mathbf{S/(n_{th} t_{ph} / t_e)} \\ \mathbf{N} &= \mathbf{n/n_{th}} \\ \mathbf{I_N} &= \mathbf{I/I_{th}} \end{aligned} \quad \textbf{... (2.3.13)}$$

where S_N, N and I_N are normalized photon number, normalized carrier number and normalized current respectively and $I_{th} = n_{th}e/t_e$ ...(2.3.14)

Now the linear gain $G_l(n) \approx G_l(n_{th}) + (dG_l/dn)(n-n_{th}) \approx 1 + (dG_l/dn)(n-n_{th})$ ...(2.3.15)

So, from (2.3.13) and (2.3.15) the linear gain G_l can be written as

$$G_l = 1 + (dG_l/dN)(N-1) \quad ...(2.3.16)$$

where ,

$$dG_l/dN = (n_{th}/g_{th})\Gamma(a/V) \quad ...(2.3.17)$$

After introducing eqns. (2.3.13), (2.3.14) in eqns. (2.3.9) and (2.3.10) finally we get the normalized and dimensionless rate eqns. for electrons and photons which are given by

$$\begin{aligned} \mathbf{dS_N/dt} &= \mathbf{(1/t_{ph})((G-1)S_N + \beta_s)} \\ \mathbf{dN/dt} &= \mathbf{(1/t_e)(I_N - N - GS_N)} \end{aligned} \quad \textbf{...(2.3.18)}$$

where $\beta_s = K_{tot} n_{sp} t_e/(n_{th} t_{ph})$

The gain can be written as

$$G(N) = [1 + (dG_l/dN)(N - 1)][1 - \kappa S_N] \quad ...(2.3.19)$$

where,

β_s = Normalized spontaneous emission rate.
κ = Normalized gain saturation coefficient.

κ is related to κ_s as

$$\kappa = \kappa_s n_{th} t_{ph} / t_e \quad ...(2.3.20)$$

Simulation of noise sources :

The noise due to spontaneous emission is realized by the Langevin noise sources F_n and F_s given by[8]

$$\begin{aligned} F_S(t_i) &= (\sqrt{2S_N(t_{i-1})t_{ph}\beta_s} / \sqrt{\Delta t}) \cdot x_e \\ F_N(t_i) &= (\sqrt{2N(t_{i-1})t_{ph}\beta_s} / \sqrt{n_{sp}\Delta t}) \cdot x_n - (\sqrt{2S_N(t_{i-1})t_{ph}\beta_s} / \sqrt{\Delta t}) \cdot x_e \end{aligned} \quad ...(2.3.21)$$

where Δt is the distance between the discreet time slots t_i and t_{i-1}.
The random variables x_e and x_n are gaussian distributed as

$$\begin{aligned} \langle x_e \rangle &= \langle x_n \rangle = 0 \\ \langle x_e^{\,2} \rangle &= \langle x_n^{\,2} \rangle = 1 \end{aligned}$$

The random variables are not correlated to each other.
After inserting the noise sources in the rate equations we can obtain final rate eqns. as

$$\begin{aligned} dS_N/dt &= (1/t_{ph})((G-1)S_N + \beta_s) + F_S(t_i)/t_{ph} \\ dN/dt &= (1/t_e)(I_N - N - GS_N) + F_N(t_i)/t_e \end{aligned} \quad ...(2.3.22)$$

Power[7],[8]

If the power output from the 1st mirror(output mirror) is *PSP1* and the power from the 2nd mirror is *PSP2* then

the total power *Ptotal* = *PSP1+PSP2*

where, $PSP2 = ((1-R_2)/(1-R_1)) \cdot \sqrt{R_1/R_2} \cdot PSP1$ ...(2.4.1)

So, the number of photons generated in the cavity corresponding to this power *Ptotal* is

$$SP = (2 \cdot Ptotal \cdot L \cdot \lambda)/(h \cdot v_{gr} \cdot c \cdot \ln(1/R_1 R_2)) \quad ...(2.4.2)$$

where, λ is the wavelength of emitted light
h is Planck's constant
c is velocity of light

The normalized photon number is

$$SN = SP/(n_{th} \cdot (t_{ph}/t_e)) \quad ...(2.4.3)$$

where $n_{th} \cdot (t_{ph}/t_e)$ describes the photon number at $I=2I_{th}$.

and the normalized current for this photon number can be written as

$$INbias = (1+SN) ...(2.4.4)$$

So the bias/on current is

$$Ibias = I_{th}(1+SN) ...(2.4.5)$$

The bias current above is the on state current when the modulation current is applied.

Laser(VCSEL)

For VCSEL the light propagation is in the perpendicular direction to the wafer surface. The light in the VCSEL bounces up and down between two highly reflecting multilayer Bragg reflectors on either side of the active layer. Most of the VCSELs are round shape to obtain highly symmetric circular output beam.

So, we have for VCSEL the radius $=r$
The effective length $= L_{eff}$
The thickness of the active region $= d$

So, the volume of the active region $V = \pi . r^2 d$ ...(2.5.0)

Here we have considered the single mode single polarization VCSEL without the effect of multilayer system.

For VCSEL we have two confinements in longitudinal and transverse directions. In transverse direction the confinement factor is taken as Γ and in the longitudinal direction the confinement factor is taken as Γ_z. Since the thickness of the active region of the VCSEL is very small compared to edge emitting laser we have Γ_z very small for VCSEL and because of full confinement in the transverse direction $\Gamma = 1$.

For VCSEL we have $d/L_{eff} \approx \Gamma_z$ ...(2.5.1)

So, for VCSEL the effective gain $g = \Gamma\Gamma_z g_{st} = \Gamma\Gamma_z (a/V)(n - n_0)$ [from eqn. (2.3.3)] ...(2.5.2)

The condition of stationary laser operation is

$$\sqrt{R_1 R_2} \exp((g - \alpha_s) L_{eff}) = 1 \qquad \text{[from eqn. (2.3.6)]}$$

...(2.5.3)

So that for VCSEL we can write the threshold gain as

$$g_{th} = \alpha_s + (1/2L_{eff}) \ln(1/R_1 R_2) = \Gamma\Gamma_z (a/V)(n_{th} - n_0)$$

...(2.5.4)

and $$n_{th} = n_0 + (1/(t_{ph} v_{gr} \Gamma\Gamma_z (a/V))) \quad ...(2.5.5)$$

Also, $$dG_l/dN = (n_{th}/g_{th})\Gamma\Gamma_z (a/V) \quad ...(2.5.6)$$

and $$\kappa_s = (1/2) h\nu v_{gr} \cdot (\ln(1/R_1 R_2)) \cdot \kappa_n / (2L_{eff}) \quad ...(2.5.7)$$

For VCSEL, the photon number in the cavity corresponding to power *Ptotal* is

$$SP = (2 \cdot Ptotal \cdot L_{eff} \cdot \lambda)/(h \cdot v_{gr} \cdot c \cdot \ln(1/R_1 R_2)))$$

These are the changes of equations which has been incorporated in simulation program for VCSEL.

the Simulation of Turn-On itter

2.1 Introduction

We have at our disposal two rate equations with noise sources and the expression for non-linear gain as follows.

$$G(N) = [1 + dG/dN(N-1)][1-\kappa S_N] \qquad ...(3.1.0)$$

$$\begin{aligned} dS_N/dt &= (1/t_{ph})((G-1)S_N + \beta_s) + (F_S(t_i)/t_{ph}) \\ dN/dt &= (1/t_e)(I_N - N - GS_N) + (F_N(t_i)/t_e) \end{aligned} \qquad ...(3.1.1)$$

The numerical solution of the coupled differential equations given by (3.1.0) has been done by ***4^th^ order Runge Kutta*** method without adaptive stepsize control using the software ***LabVIEW***.

The random numbers x_e and x_n in the Langevin noise sources F_s and F_n are generated by standard gaussian noise sources from LabVIEW standard tool. These Langevin noise sources are added to the rate equations to simulate the spontaneous emission noise.

A subprogram which generates the necessary parameters for solving the rate eqns. has been developed. This parameter file needs some basic parameters of the laser as input to give some output parameters which are taken as the input of the main program.

The laser characteristics graph has been plotted first by changing the power output and observing the corresponding bias current.

Initially the bias current is applied to make the laser in steady state after few oscillation. This bias current is the on-current I_{on} when modulation current is applied. For a particular off-current I_{off} different on-current i.e different output power P_{on} at the on state of laser is applied. Also for a particular on-current different I_{off} is applied to observe the effect of off-current. First the *1010 pattern* is applied and then the *pseudo random pattern* is applied to observe the bit pattern effect.
For simulation with the VCSEL provided by Prof. Ebeling, University of Ulm, Germany, the data rate taken for simulation of jitter is *160 Mbits/s* to match with the experimental results. Also to observe the effect of high data rate on jitter the simulation is carried on for *1Gbits/s*. The duration of a time slot (i.e step size for numerical solution) Δt =1e-12 is taken for convenience. The total number of bits taken for simulation are 5000. The photon turn on dela is calcu ated whenever the current changes from off state to on state So during the time whe

5000 bits are transmitted many turn on delays (t_{on}) are obtained ***The probability density function (PDF)*** of these t_{on} s is plotted The ***mean t_{on}*** is calculated and the RMS of this PDF gives the ***simulated jitter.***

Also ***the average relaxation oscillation frequency f_r*** is measured automatically in the main program by using various LabVIEW tools.

In simulation the values of jitter and f_r are calculated for several on states i.e for several output power P_{on} with zero bias and compared with the *experimental results* as well as with the *theoretical model*[2] and then the simulation is carried out with different off-states.

Then the graph between rms turn-on jitter and relaxation resonance frequency is plotted to compare with the theoretical model as well as with the experimental measurements.

In this simulation of turn on jitter and calculation of f_r for Ebeling VCSEL some parameters have been chosen logically apart from some standard supplied parameters of the laser to match with the experimental results.

The parameters which are supplied for Ebeling VCSEL are *radius(r), length of the active region (d), effective length (L_{eff}), wavelength of the emitted light (λ),group velocity(v_{gr}).*

The parameters which are chosen are *electron life time (t_e) ,photon life time (t_{ph}), reflectivity of the mirrors (R_1,R_2)* so that a good fit with the experimental results and theoretical model can be achieved.

This type of simulation is called ***simulation verification*** *which approximately represent the real world system.* In this simulation model some simplifying assumption has been made e.g, *single mode single polarization VCSEL without considering the multiple quantum well effect.*

simulation program - Description

flow diagram of the program

agram of the program which has been developed by LabView is shown belo

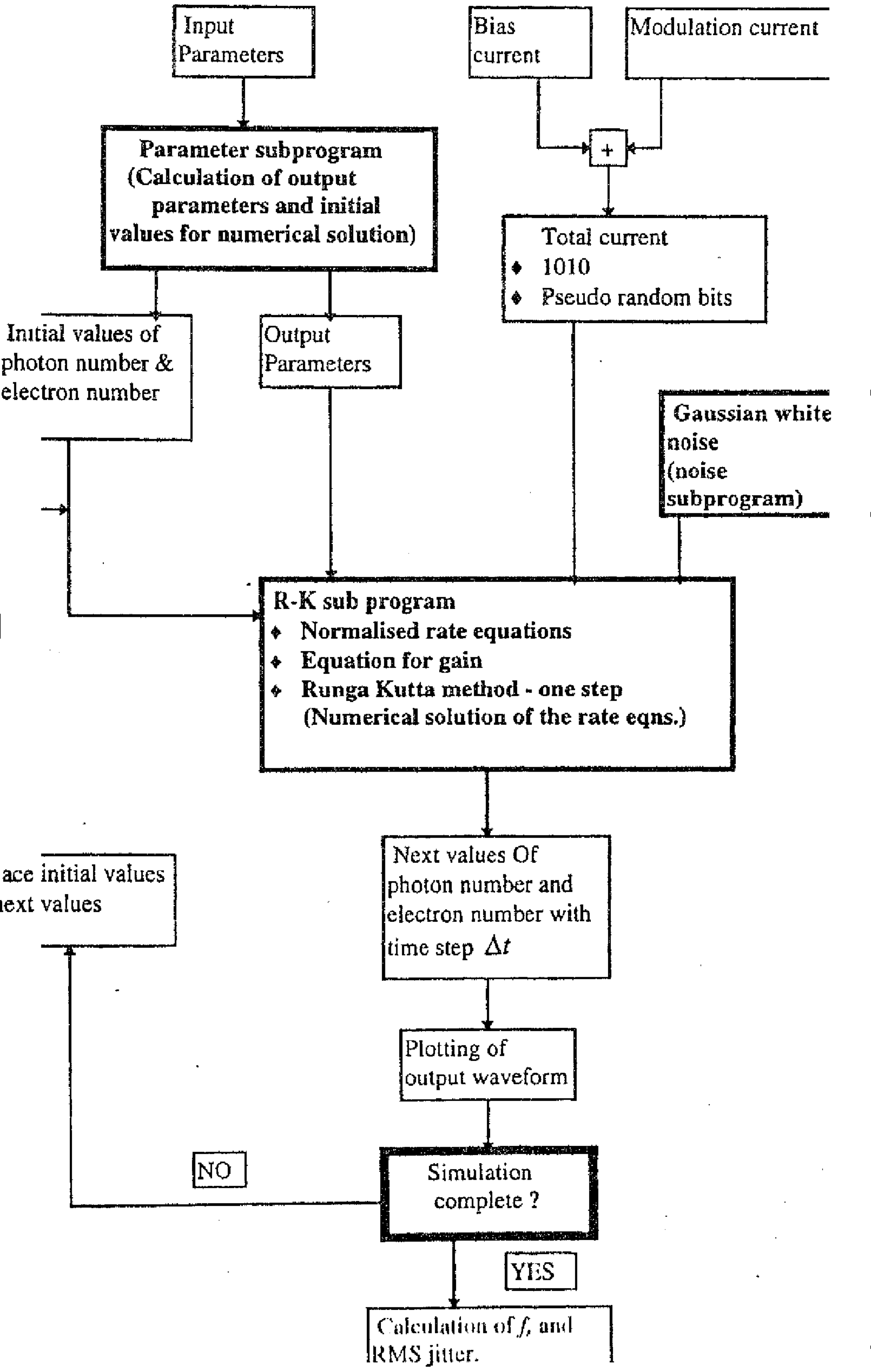

2 2.2 The parameter subprogram

When the main program is runned, it calls the **parameter subprogram(parameter.** that user can give necessary input parameters of the particular VCSEL to calculate s derived parameters which are necessary for solving the rate equations numerically a simulation of jitter. The input parameters of the Ebeling VCSEL which have been u: LabVIEW subprogram **parameter.vi** for the simulation are given below:

- *Output power through mirror1(PSP1=Pon)=variable*
- *Wavelength(lamda)=870nm*
- *Radius of the VCSEL(rad)=2μm*
- *Thickness of the active region(d)=24nm*
- *Effective length(Leff)=3.5μm*
- *Group velocity of the optical wave in the active region(vgr)=8.3e7m/s*
- *Photon life time(tph)=4.4ps*
- *Electron life time(te)=1.2ns*
- *Carrier number at population inversion(n0)=6.6e5*
- *Reflectivity of mirror 1(R1)=0.99*
- *Reflectivity of mirror2(R2)=0.99*
- *Gain proportional coefficient(dgstdn=a)=2.0e-20*m^2
- *Time slot interval(Step size)(dx)=1ps*
- *Gain compression coefficient related to optical power(kp)=25*W^{-1}
- *Longitudinal confinement factor(gamma=*Γ_z*)=6.8e-3*

With these input parameters some output parameters are calculated which are neces: the main program to run. These parameters are given below:

- *Normalized bias/on current corresponding to the power PSP1(INbias)=variable*
- *Normalized photon number in on state corresponding to the power PSP1(SN-on)* *value of normalized photon number needed for simulation(SN)=variable*
- *Normalized value of initial electron number(N)=1*
- *Photon life time(tph)=4.4ps*
- *Electron life time(te)=1.2ns*
- *Starting value of independent variable(time) for numerical solution(x)=0*
- *Time slot interval(Step size)(dx)=1ps*
- *Normalized gain saturation coefficient(k)=1.666e-2*
- *Normalized spontaneous emission rate(betas=*β_s*)=8.9933e-5*
- *dG/dN=1.1087*
- *Threshold carrier number(nth)=6.7323e6*
- *Threshold gain(gth)=2.7382e3*m^{-1}

The above derived parameters are calculated in the parameter subprogram accordin equations described in chapter 2.3.
When the main program is executed first the parameter subprogram runs in a numb sequence to calculate output parameters which are subsequently fed to the **R-K subprogram(newRK4.vi)**. Initially the laser is assumed to be in steady state with t power(PSP1) so that the initial (steady state) value of electron number (N=1) and p number(SN-on)needed for numerical solution of the rate equations are calculated a the R K subprogram So the bias to the aser is given from the parameter file

The VCSEL supplied by Prof Ebeling has multilayer system For emission near 870nm wavelength the one wavelength thick inner cavity contains three each 8 nm thick GaAs quantum wells. So the thickness of the active medium is taken as d=24 nm. Since longitudinal confinement factor $\Gamma_z \approx d/L_{eff}$ and L_{eff}=3.5μm, so $\Gamma_z = 6.8e\text{-}3$ has been taken correctly. The radius of the VCSEL is supplied as 2 μm. *In the simulation model of the VCSEL the experimentally obtained threshold current I_{th} =0.9 mA and slope of the laser characteristics (dP/dI=0.775) above threshold are matched first by the following formulas*

$$I_{th} = n_{th} e/t_e \quad ...(3.2.2.1)$$

where $$n_{th} = n_0 + (1/(t_p v_{gr} \Gamma_z (a/V))) \quad ...(3.2.2.2)$$

and $$dP/dI = (h v_{gr} c \ln(1/R_1 R_2)/4 L_{eff} \lambda e) \cdot t_p \quad ...(3.2.2.3)$$

where $R_1 = R_2 = 0.99$ and t_p=4 ps , t_e=1.2 ns are taken.
A separate program (**fr.vi**) has been developed to calculate *Ibias*, f_r and I_{th} by the following formulas:

$$\begin{aligned} Ibias &= (n_0 e/t_e) + (e/t_p t_e v_{gr} \Gamma_z (a/V)) + (4e(PSP1) L_{eff} \lambda / t_p h v_{gr} c \ln(1/R_1 R_2)) \quad ...(3.2.2.4) \\ &= C_1/t_e + C_2/t_p t_e + C_3 (PSP1)/t_p \end{aligned}$$

[from equations (2.4.1) to (2.4.5) in chapter 2]

where
$$\begin{aligned} C_1 &= n_0 e = 1.056e-13 \\ C_2 &= e/v_{gr} \Gamma_z (a/V) = 4.29e-24 \\ C_3 &= 4 e L_{eff} \lambda / h v_{gr} c \ln(1/R_1 R_2) = 5.9e-12 \end{aligned}$$

and
$$\begin{aligned} f_r &= (1/2\pi) \cdot \sqrt{\Gamma_z v_{gr} (a/V)/e} \cdot \sqrt{Ibias - (n_{th} e/t_e)} \quad ...(3.2.2.5) \\ &= C_5 [\sqrt{Ibias - n_{th} e/t_e}\,] \end{aligned}$$

[from the basic equation $f_r = (1/2\pi) \cdot \sqrt{(1/n_{th})(dG/dN)(I_{bias} - I_{th})/e t_{ph}}$]

where $$C_5 = (1/2\pi) \cdot \sqrt{\Gamma_z v_{gr} (a/V)/e} = 7.68e10$$

and I_{th} is given by the formula (3.2.2.1) using n_{th} (3.2.2.2).

In the program **fr.vi** a range of values of t_{ph} (from 3.5 ps to 4.4 ps) and a range of values of t_e (from 0.5 ns to 2.3 ns) has been used to calculate f_r ,*Ibias* and I_{th} for a particular power PSP1 and those values of t_{ph} and t_e are taken finally which gives a good fit with the experimental values of f_r ,*Ibias* and I_{th}.

Finally the values of photon life time t_{ph} and electron life time t_e are taken as 4.4 ps and 1.2 ns respectively with which the simulation results are matching well with experimental results. K_p is chosen as 25 for sufficient damping to limit the oscillation.

2.2.3 The noise subprogram

In the noise subprogram (**noi.vi**) the Langevin noise sources F_n and F_s are generated to add these functions to the rate equations in the main program. The random variables x_e and x_n are generated in the main program by standard LabVIEW gaussian noise generators with standard deviation equal to 1 and these are fed in the noise subprogram. For every step of solving the rate equations numerically one value of noise is generated and applied to the rate equations. These noise sources are added to simulate the spontaneous emission noise so that one can observe fluctuation of turn on delay and jitter can be simulated.

2.2.4 The R-K subprogram

The **R-K subprogram(newRK4.vi)** consists of the following subprograms :

- **newfxy.vi**
- **newarr.vi**
- **newdSNdt_dNdt.vi**
- **newGN.vi**

In the R-K subprogram the ***4th order Runge-Kutta*** method is applied to solve the rate equations simultaneously. In this subprogram one step R-K method has been done to calculate the new values of photon number(SN) and electron number(N) after giving the initial values of these using step size $\Delta x = 1ps$. The R-K method can be described as following:

If we have a set of N first order ordinary differential equations as[9]

$$dy_i(x)/dx = f_i(x, y_1, \ldots\ldots y_N) \qquad \text{where } i = 1, 2, \ldots\ldots N$$

Usually, it is the nature of the boundary conditions that determines which numerical methods will be feasible to solve the equations. In the *initial value problems* all the y_i are given at some starting value x_s, and it is desired to find the y_i's at some final point x_f, or at some discrete list of points.

One practical numerical method for solving initial value problems is *Runge-Kutta method* according to which for any equation if x_n and y_n are the previous values and if the value of x_n is increased by step size h ($x_{n+1} = x_n + h$) then we can calculate the new value of y_n as

$$y_{n+1} = y_n + K_1/6 + K_2/3 + K_3/3 + K_4/6$$

where,
$$K_1 = h \cdot f(x_n, y_n)$$
$$K_2 = h \cdot f(x_n + h/2, y_n + K_1/2)$$
$$K_3 = h \cdot f(x_n + h/2, y_n + K_2/2)$$
$$K_4 = h \cdot f(x_n + h, y_n + K_3)$$

The 4[th] order Runge-Kutta method requires four evaluations of the above right-hand side per step h.
Here only two rate equations has been solved, so $N=2$ *and* $y_1=SN$ *and* $y_2=N$, where SN and N are normalized photon number and normalized electron number respectively and $h = \Delta x$.

In the subprogram **newGN.vi** the equation for nonlinear gain G(N) (eqn.2.3.19) is constructed by standard LabVIEW tools which is required in the rate equations.
In the subprogram **newdSNdt_dNdt.vi** the rate equations for photon and electron has been constructed with the noise sources added from the noise subprogram and the bias current as well as the modulation current is applied here from the main program. The **newGN.vi** is a subprogram of this program.

In the subprogram **newfxy.vi** the photon number SN and electron number N have been put in an array and applied in the subprogram **newarr.vi** which separates the elements in the array and the separated elements (SN,N) are then put in the subprogram **newdSNdt_dNdt.vi**.

In the program **newRK4.vi** the program **newfxy.vi** has been used as a subprogram to solve the rate equations numerically by R-K method.

2.2.5; The main program

The main program **VCSELPRS2.vi** consists of the following subprograms.

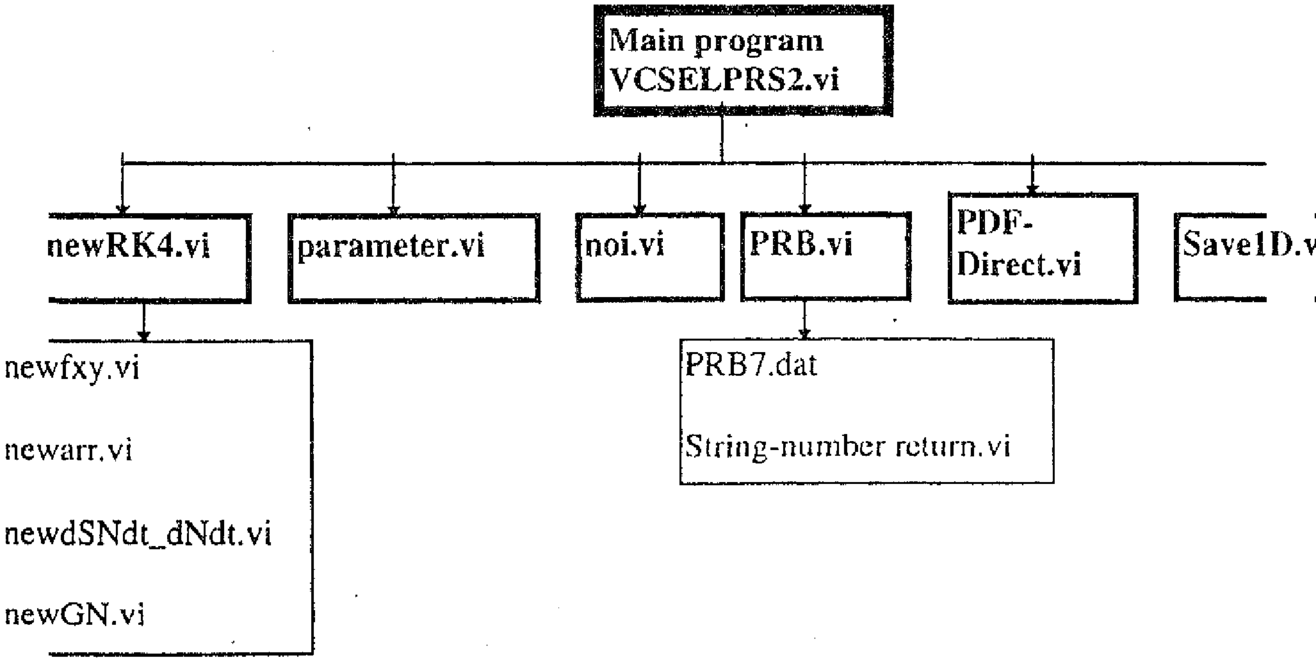

When the main program is executed it takes first the parameters necessary from the paramete file to solve the rate equations Initially the laser is biased with some bias current corresponding to the power PSP1 and after the laser comes to the steady state the modulation current is applied from the main program where the on-state is taken as the bias level. The simulation is carried on for several off state. Two types of modulation current is applied -1010 pattern and pseudo-random pattern. The subprogram **PRB.vi** generates the pseudo-random bits taken from the data file **PRB.dat.** From the front panel of the program the data rate is given and corresponding bit duration is calculated as well as the number of sampling points during one bit period are calculated. *The program is executed for several thousand bits and the variation of normalized carrier numbers and normalized photon numbers are plotted with time with the modulation current.* In every sampling step of numerical solution of the equations one value of noise from the gaussian noise subprogram is added to the equations. Also the *turn-on delay* is calculated when the laser is switched from off-state to on-state and the turn on delay is taken as the time when the photon number reaches the steady state value first during turn-on event. The *mean turn-on delay* as well as *probability density function(PDF)* of the turn-on delay is calculated in the subprogram **PDF-Direct.vi.** The *rms jitter* is also calculated in the same subprogram. The relaxation resonance frequency f_r is also calculated in every on-state and the average f_r is calculated. The main program is executed for several on-state power PSP1.

r 3

ation results and conclusions

haracteristics

ying the modulation current the characteristics of Ebeling VCSEL is m
g the parameter file. After introducing the parameters of the VCSEL w
output power vs. bias current by changing different power PSP1[Table
ics graph obtained is matching well with the experimental graph as sho

d P-I characteristics of Ebeling VCSEL(4μm)	
lamda=870nm	
Current Ibias(A) (measured)	**Current Ibias(A) (simulated)**
2.50E-03	2.47E-03
2.40E-03	2.38E-03
2.30E-03	2.31E-03
2.20E-03	2.22E-03
2.10E-03	2.13E-03
2.00E-03	2.03E-03
1.90E-03	1.93E-03
1.80E-03	1.83E-03
1.70E-03	1.72E-03
1.60E-03	1.61E-03
1.50E-03	1.50E-03
1.40E-03	1.40E-03
1.30E-03	1.29E-03
1.20E-03	1.19E-03
1.10E-03	1.10E-03
1.00E-03	1.01E-03
9.00E-04	9.25E-04
8.00E-04	9.08E-04
7.00E-04	9.06E-04
6.00E-04	9.04E-04
5.00E-04	9.03E-04
4.00E-04	9.01E-04
3.00E-04	9.00E-04
2.00E-04	8.98E-04
1.00E-04	8.97E-04

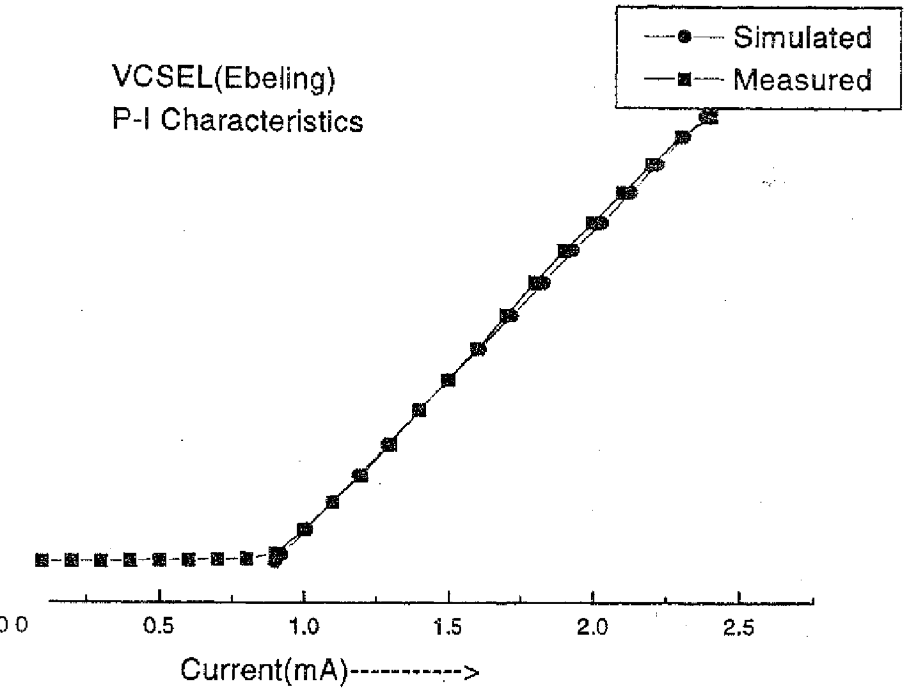

4.1.1 **P-I Characteristics of Ebeling VCSEL**

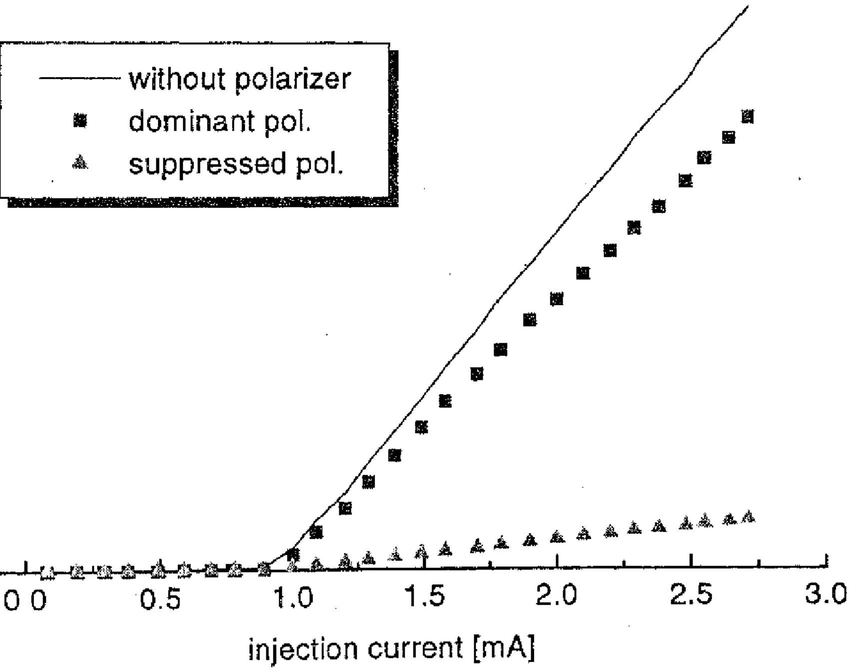

4.1.2 **Experimentally obtained P-I characteristics of Ebeling VCSEL.**

mu ation it s assumed t at the VCSEL has on y one po arization But from th
nt measurements (fig 4 1 2) it has been foun t t the Fbe ing VCSEL h s
ions- one dominant and other is suppressed polarization which has significant
ing turn-on time under zero-bias condition(or below threshold)[10]. But from
istics graph (fig 4.1.2) obtained experimentally it shows the power of the sup
ion is very small compared to the dominant one. So although in simulation it i
that there is only one polarization , the simulated P-I curve may be matched v
experimental one.

mulation of turn-on jitter

to investigate the turn-on behaviour of the VCSEL the modulation current is a
e experimental measurements have been done with **bitrate 160Mbits/s with z**
l 1010 bit pattern, the same data rate has been used in simulation also to com
measurement results. Additionally, the simulation has been done for **different**
observe the effects of off-state on jitter. The sampling time interval for solvin
ial equation is taken as 1 ps.

Table 2: Results obtained by simulation for zero biased VCSEL
Data rate=160 Mbit/s
Bit pattern=1010

POWER(W)	fr(GHz) measured	fr(GHz) simulated	JITTER(ps) measured	JITTER(ps) simulated
7.50E-04	2	2.18	25.39	22.34
8.00E-04		2.25		21.3
9.50E-04		2.44		19.69
1.11E-03	2.77	2.64	17.16	17.16
1.34E-03	2.94	2.91	13.19	15.5
1.50E-03		3.06		14.4
1.88E-03	3.33	3.48	7.78	12.6
2.29E-03	3.7	3.96	5.75	11

shows the measured rms turn-on jitter vs. the relaxation resonance frequenc
with the results found by numerical simulation of the rate equations for *zero b*
1010 pattern) at 160 Mbit/s[Table 2]. It can be seen, that the turn-on jitter dec
asing values of f_r. By comparison with eqn. (2.2.5) in chapter 2 , we find that
g barrier" $\langle S_c \rangle$ for this specific laser is about 188. As evident the simulation
od agreement with the measurement (f_r <3 GHz) and theoretical model. Abov
at sufficient high on-state the laser is multimode as obtained experimentally a
tion of jitter vs f as obtained from measurements is not matching with the s

e results from the simulation is matching with the theoretical graph sinc
odel is derived only for single mode VCSEL. Above f_r =3 GHz the exis
ersal modes yields a reduction of turn-on jitter due to the increased deg
the VCSEL to reach the stationary value at the on state. However, if the
, the mode partition noise must be taken into account yielding an increa

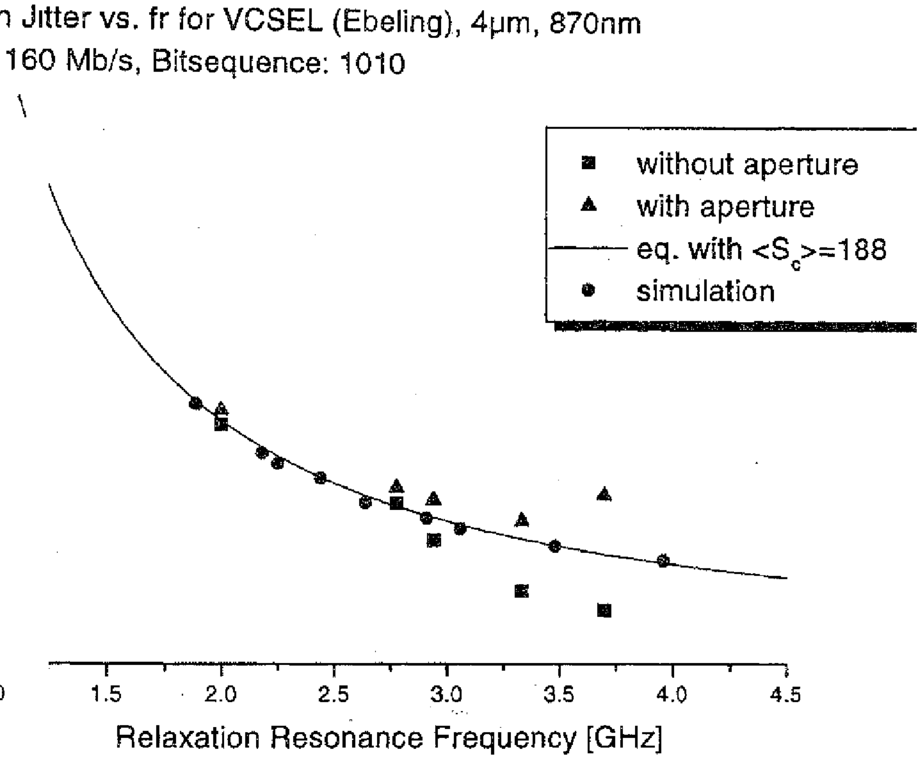

Fig 4.2.1 **Turn-on jitter vs. relaxation resonance frequency**

, ***the dependence of turn-on jitter on the off-state*** has been investigated
delay pdf according to eqn.(2.2.5) should be independent of the off-state
This has been confirmed experimentally for edge-emitting laser[2]and f
imulation result shows the same behaviour as it is expected. The jitter i
as the off-state is below threshold.
the turn-on jitter decreases as obtained from simulation results as it is ex
ulated emission is dominant above threshold compared to spontaneous
ble 3].

Table 3: Simulation results for different off-states

POWER(W)	JITTER(ps) simulated INOFF=0	JITTER(ps) simulated INOFF=0.9	JITTER(ps) simulated INOFF=1.2
7.50E-04	22.34	22.41	12.5
8.00E-04	21.3	20.64	11.5
9.50E-04	19.69	19.06	10
1.11E-03	17.16	16.74	8.6
1 34E-03	15 5	16 63	7 3

n resu.ts s..,ws th.t relaxatio.i resonance frcquency docs not depends or

Calculation of relaxation resonance frequency for different off-state

W)	fr(GHZ) simulated INOFF=0	fr(GHz) simulated INOFF=0.9	fr(GHz) simulated INOFF=1.2
.50E-04	2.18	2.18	2.4
.00E-04	2.25	2.25	2.48
.50E-04	2.44	2.44	2.69
.11E-03	2.64	2.64	2.89
.34E-03	2.91	2.9	3.17

S

results are in good agreement with the measurements and with theoretic

GHz the single mode simulation results is not matching with the al results since the VCSEL is multimode.

independent of off-state as long as the off-state is below threshold.

ate is above threshold the jitter decreases as expected.

resonance frequency does not depend on off-states

of bit-rate and bit pattern on jitter

ulation of jitter at different data rates and bit patterns with zero bi

)	JITTER(ps) 160 Mbit/s 1010 pattern	JITTER(ps) 160bit/s pseudo random	JITTER(ps) 1Gbit/s 1010 pattern	JITTER(ps) 1Gbit/s Pseudo-rand
4	27.52	27.4	26.12	4
4	21.3	21.81	21.97	9
3	17.16	17.17	18.42	
3	14.4	14.35	14.52	
3	11	11.17	11.11	

VCSEL(Ebeling)

Data rate = 160Mbits/s

lamda=870nm

1010 pattern

Ioff=0

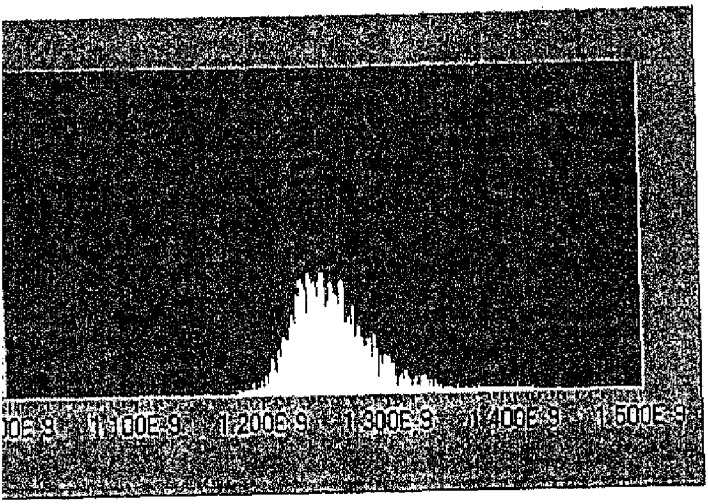

Pon=5.32e-4W
jitter=27.516 ps

Fig 4.3.1 a

Turn-on delay(s)

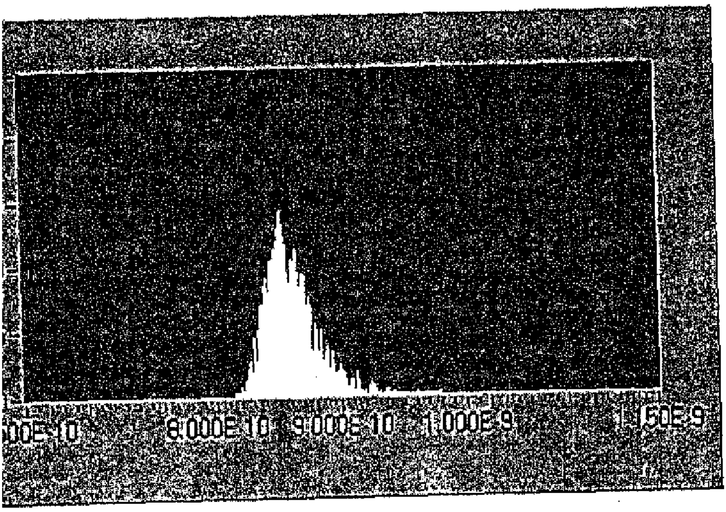

Pon=0.95e-3W
jitter=19.68 ps

Fig 4.3.1 b

Turn-on delay(s)

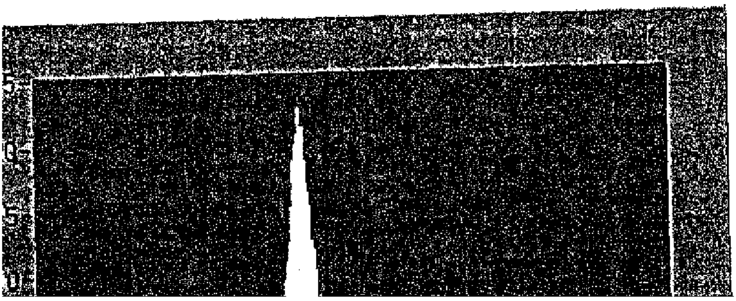

Pon=2.29e-3W
jitter=11 ps

Fig 4.3.1 c

d is 1Gbit/s(1010 pattern) to observe the behaviour of jitter on data rat
coming almost same as that of when the data rate is 160 Mbit/s[Table

ndom pattern is applied at 1 Gbits/s due to bit pattern effect the jitter
ly[Table 5]. But the PDF graph obtained is not the same nature as that
g 4.3.1 a,b,c). This is because the turn-on delay depends on the numbe
fore a one(1) comes. For pseudo random bit pattern this happens
ore the nature of the PDF graph obtained (Fig 4.3.2) is quite different
ear from the distribution graph that the probability of a single zero bef
n the probability so that two zeros come and so on. The values of jitte
ition results do not give the actual value of jitter since the PDF graph h
it gives the measure of fluctuation of turn-on delay. So qualitatively w
jitter increases for pseudo-random pattern at high data rate.

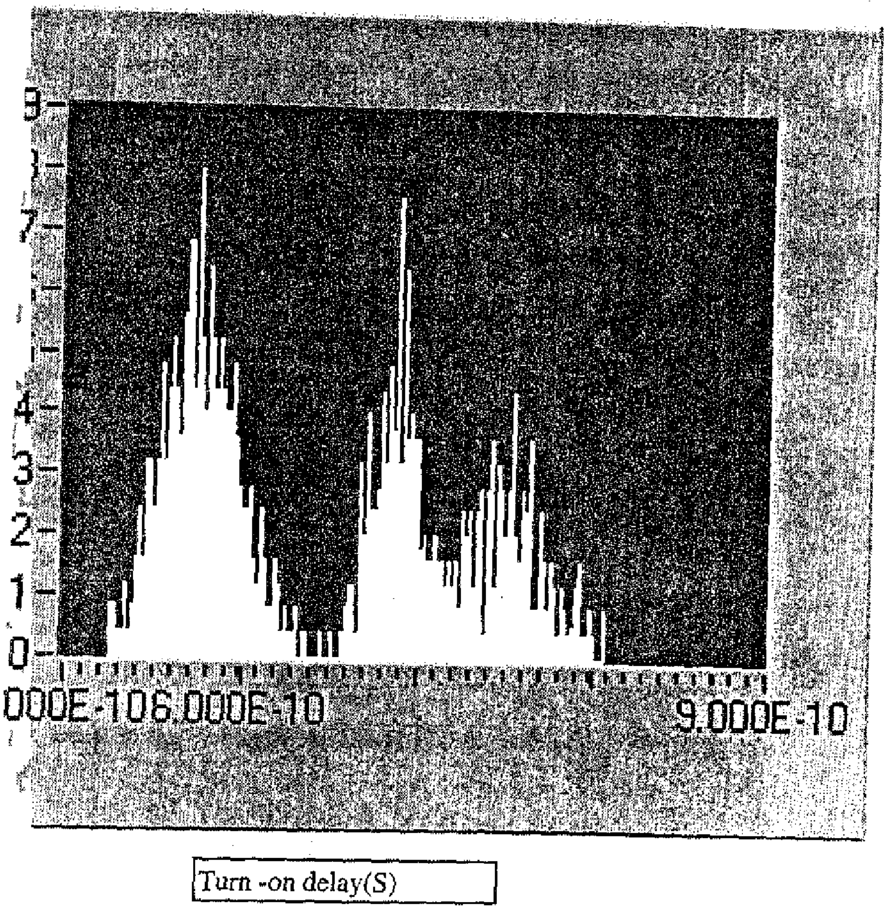

2 **PDF of turn on delay for pseudo random bit pattern at 1 Gbi**

:

rn effect comes at high data rate.

- Jitter is independent of bit rate as long as the bit pattern is 1010
- Jitter increases due to bit pattern effect at high data rate.
- The nature of variation of jitter with on-states is different for high data rate with pseudo random bit pattern.

4 The practical relevance and the utility of the numerical mulation model:

This simulation model approximately represents the real world system.

It is important to investigate the turn-on jitter(due to spontaneous emission and bit pattern effect) since it causes the increase of BER at gigabit data rate in optical communication system. With this simulation model we can investigate the turn on behaviour of any single mode-single polarization VCSEL after introducing the parameters of the VCSEL in the program without performing the experiments.

The simulation results here matches well with the results obtained form the theoretical model described in [2]. Since the simulation is performed by numerically solving the basic rate equations it actually verifies that analytical model is correct.

From the simulation results we get how the jitter varies with the on-state level of the modulation current for a zero biased laser. So for high data rate to obtain less BER we can choose at what range of on-level the laser should be operated to get BER less than 10^{-9} which is the tolerable BER for communication purpose.
In simulation we can plot how the photon number and carrier number varies with the variation of current. Also we can observe the relaxation oscillation and we can investigate what parameters affects the oscillation(e.g gain compression coefficient k_p (fig 4.4.1)). It can be observed that if k_p is increased the oscillation decreases and for k_p =25 W^{-1} the oscillation is quite matching with the experimentally obtained oscillation. So we can say for this laser the value of k_p =25 W^{-1} approximately.

In simulation by changing bit rate we can investigate the effect of bit rate on jitter and also we can measure upto what data rate the laser can operate because the upper limit of bit rate will depend on electron and photon turn-on delay also for zero biased laser. By applying high data rate(1 Gbits/s) the effect of bit rate on jitter has been investigated. It shows that jitter does not depends on bit rate as long as 1010 bit pattern is applied. For pseudo randon the jitter changes with bit rate. Higher the bit rate high is the jitter.

Here the simulation model has been done for source only. In optical communication systen we can simulate the transmission channel as well as the receiver also. Then one can connect different module by applying the output of one to the next and the whole communication system can simulated to investigate the behaviour of it.
The eye diagram can be plotted by overlapping successive bits in this model and with the help of this diagram the BER can be measured for a particular data rate and for a particular on-state.

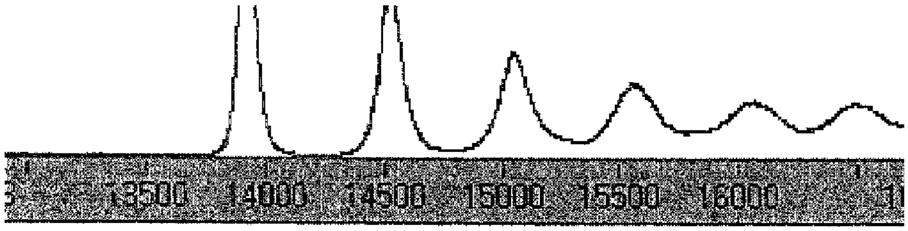

k_p=3.5 W^{-1}

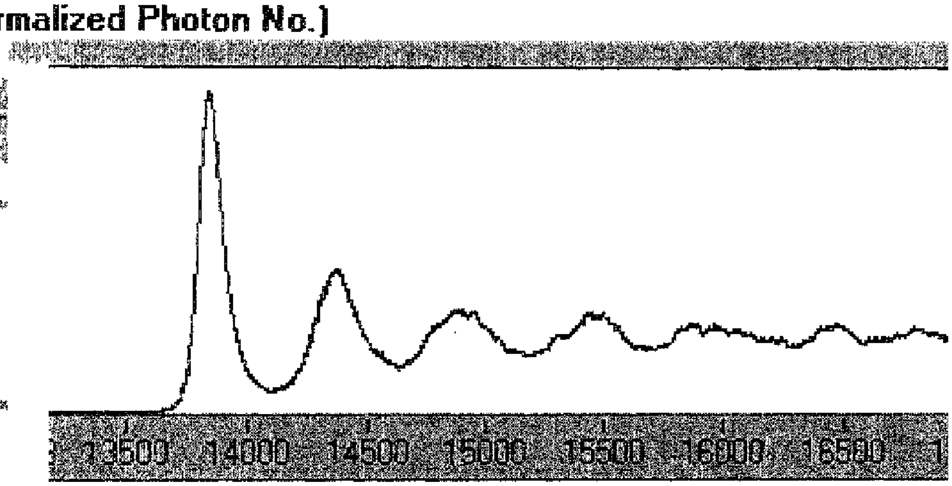

k_p=25 W^{-1}

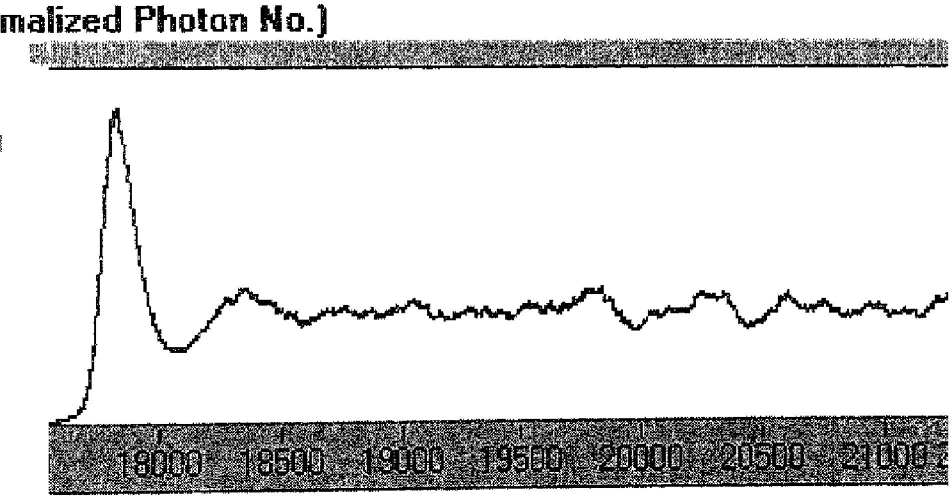

k_p=50 W^{-1}

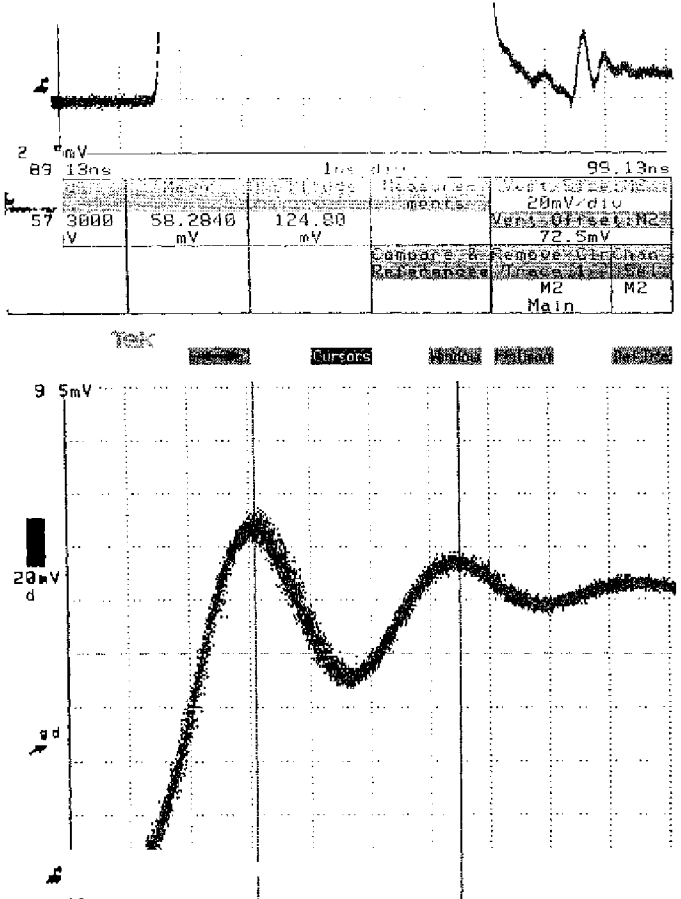

89 13ns
1ns/div
99.13ns
58.2840
mV
124.80
mV
ments
20mV/div
Vert Offset M2
72.5mV
Compare & References
Remove/Clr Trace 1-2
Chan Sel
M2
Main
M2
Tek
Cursors
20mV

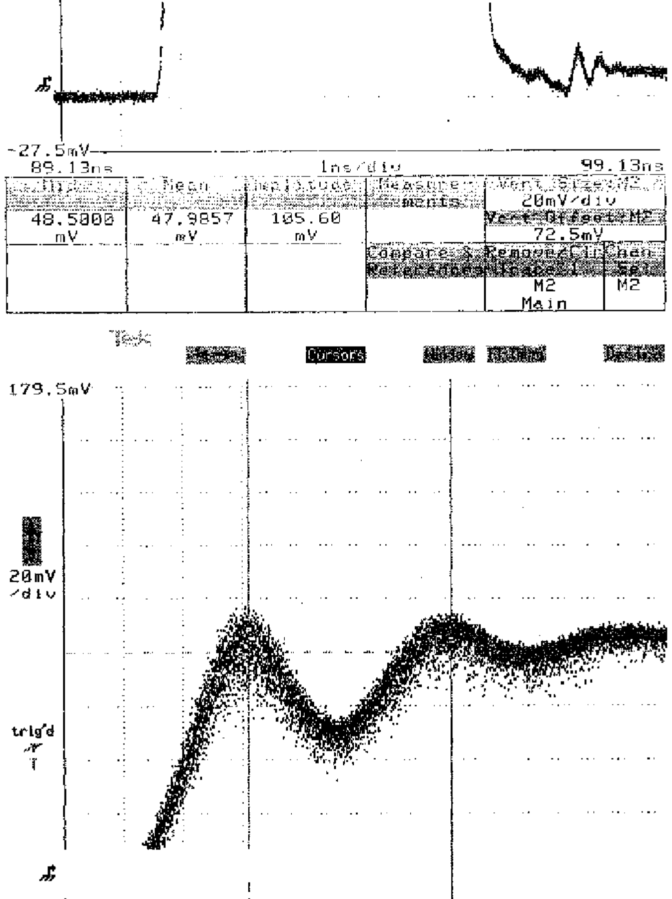

-27.5mV
89.13ns
1ns/div
99.13ns
Mean
48.5800
mV
47.9857
mV
105.60
mV
ments
20mV/div
Vert Offset M2
72.5mV
Compare & References
Remove/Clr Trace 1
Chan Sel
M2
Main
M2
Tek
Cursors
179.5mV
20mV
/div
trig'd

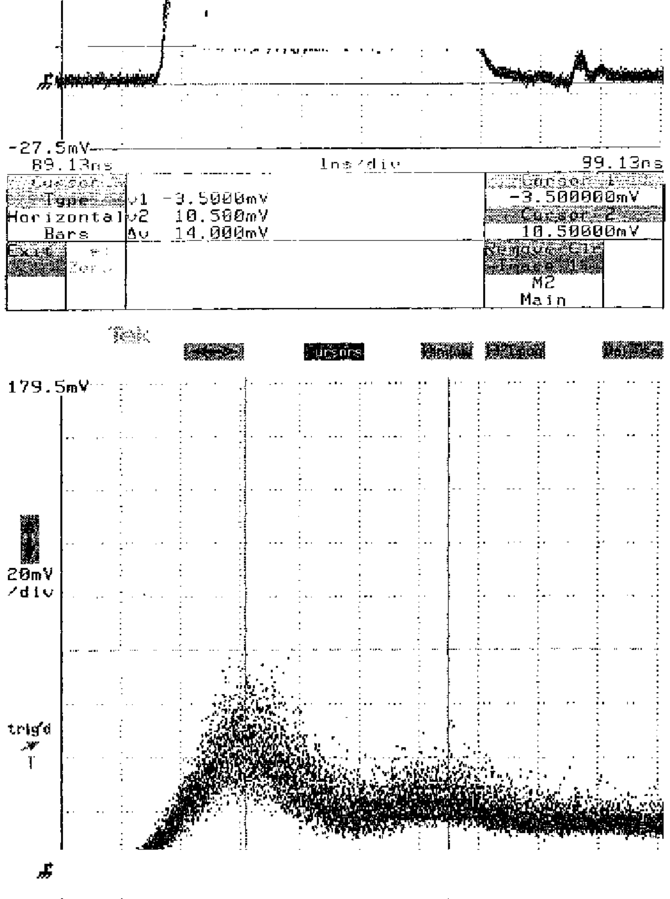

-27.5mV
89.13ns
1ns/div
99.13ns
Cursor
Type
Horizontal
Bars
v1 -3.5000mV
v2 10.500mV
Δv 14.000mV
Cursor 1
-3.500000mV
Cursor 2
10.50000mV
Exit
M2
Main
Tek
Cursors
179.5mV
20mV
/div
trig'd

- Also the effect of different bit pattern on jitter can be observed in this simulation mo
When the pseudo random pattern is applied the simulation results shows that jitter increases significantly due to bit pattern effect especially for zero-biased operation effect has been verified experimentally also. Although the effect of bit pattern effect significant at very data rate(Gbits/s).

- The simulation model can be modified and the work can be extended further for two polarization multimode VCSEL.

REFERENCES

[1] Torsten Wipiejewski," Siemens Components", 4/98, page-23.

[2] K. Obermann, S. Kindt, and K. Petermann, " Turn-On Jitter in Zero-Biased Single-Mode Semiconductor Lasers", *IEEE Photon. Technol. Lett.*, vol. 8, No.1, pp. 31-33, January 1996.

[3] T. Czogalla and K. Petermann, " Turn-On Jitter in Zero-Biased Single-Mode Vertical Cavity Surface Emitting lasers" , *Proc. Summer Topical Meeting '97, Montreal, Canada,* 1997.

[4] A. Mecozzi, A. Sapia, P. Spano, and G. Agrawal, " Transient multimode dynamics in nearly single mode lasers," *IEEE J.Quantum Electron.*, vol. 27, pp. 332-343, 1991.

[5] T. Stephens, K. Hinton, T. Anderson, and B. Clarke," Laser turn-on delay and chirp noise effects in Gb/s intensity-modulated direct-detection systems," *J. Lightwave Technol.*, vol. 13, pp. 666-674, 1995.

[6] R. S. Tucker, " High-speed modulation of semiconductor lasers", *J. Lightwave Technol.*, vol.3, pp. 1180-1192, 1985.

[7] K. Petermann, " Laser Diode Modulation and Noise", Dordrecht, The Netherlands, Kluwer Academic Publishers, 1988.

[8] Nikolaus Schunk," Rauschverhalten von halbleiterlasern bei Optischer Rückwirkung", *Dissertation work, Technical Univ., Berlin* 1989.

[9] W. H. Press, A. Teukolsky, W. T. Vetterling and B. P. Flannery, *Numerical Recipies in C,* Cambridge University Press, New York, 1992.

[10] L. Zei, K. Obermann, K. Petermann, D. Wiedenmann, K. J. Ebeling, " Turn-On Jitter Of Zero-Biased Polarization Controlled Single-Mode VCSELs", *24th European Conference on Optical Communication(ECOC' 98),* Sep. 20-24,1998 Madrid, Spain.

Appendix

LabVIEW simulation programs

1. Main program (VCSELPRS2.vi)

2. Parameter subprogram (parameter.vi)

3. R-K subprogram (newRK4.vi)

   a) newfxy.vi
   b) newarr.vi
   c) newdSNdt_dNdt.vi
   d) newGN.vi

4. Noise subprogram (noi.vi)

5. PDF subprogram (PDF-Direct.vi)

6. Program for selection of parameters t_e, t_p (fr.vi)

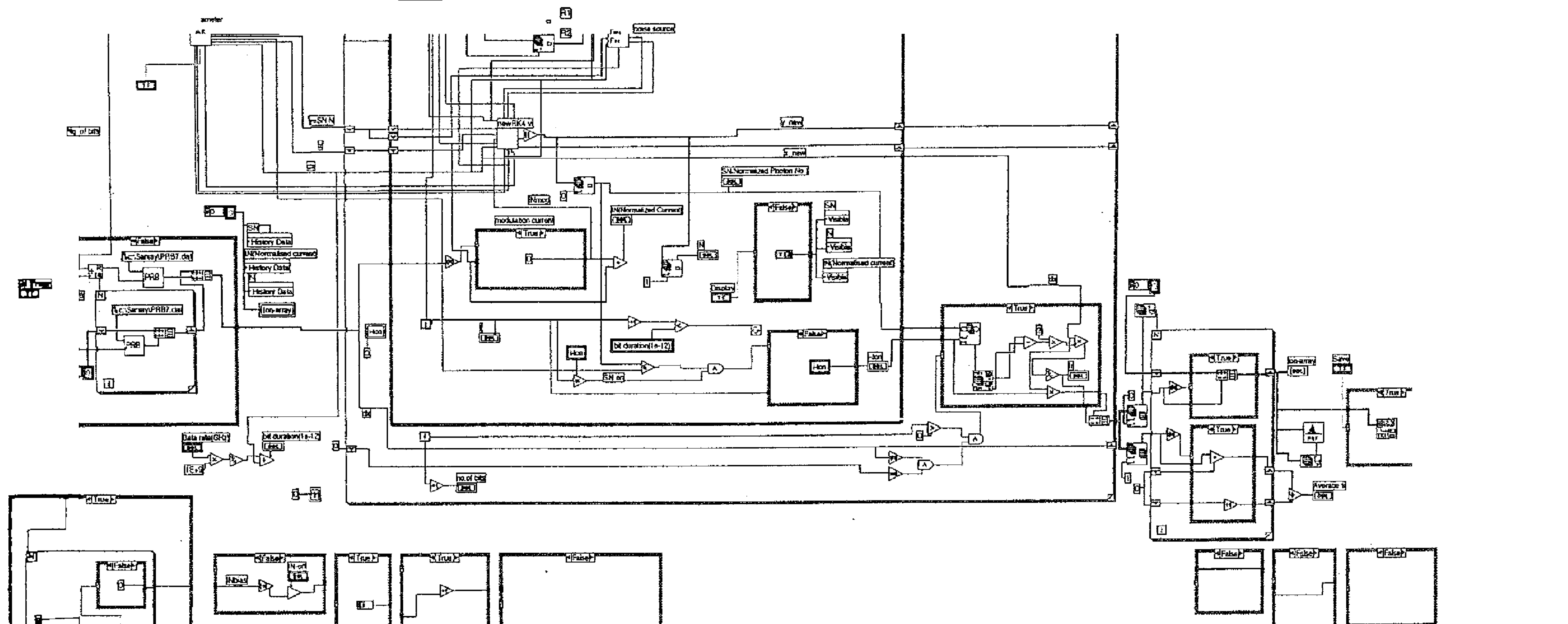

ameter
noise source
new RK4.vi
y_new
x_new
SN Normalized Photon No.
modulation current
N\Normalized Current
Nmod
Display
N\Normalised current
Visible
bit duration(1e-12)
SN on
Hon
History Data
c:\Sanjay\PRB7.dat
Ion-array
Data rate(GHz)
no. of bits
No. of bits
Nbias
N-off
Save
Average

2 98 at 14 27
at 18.31

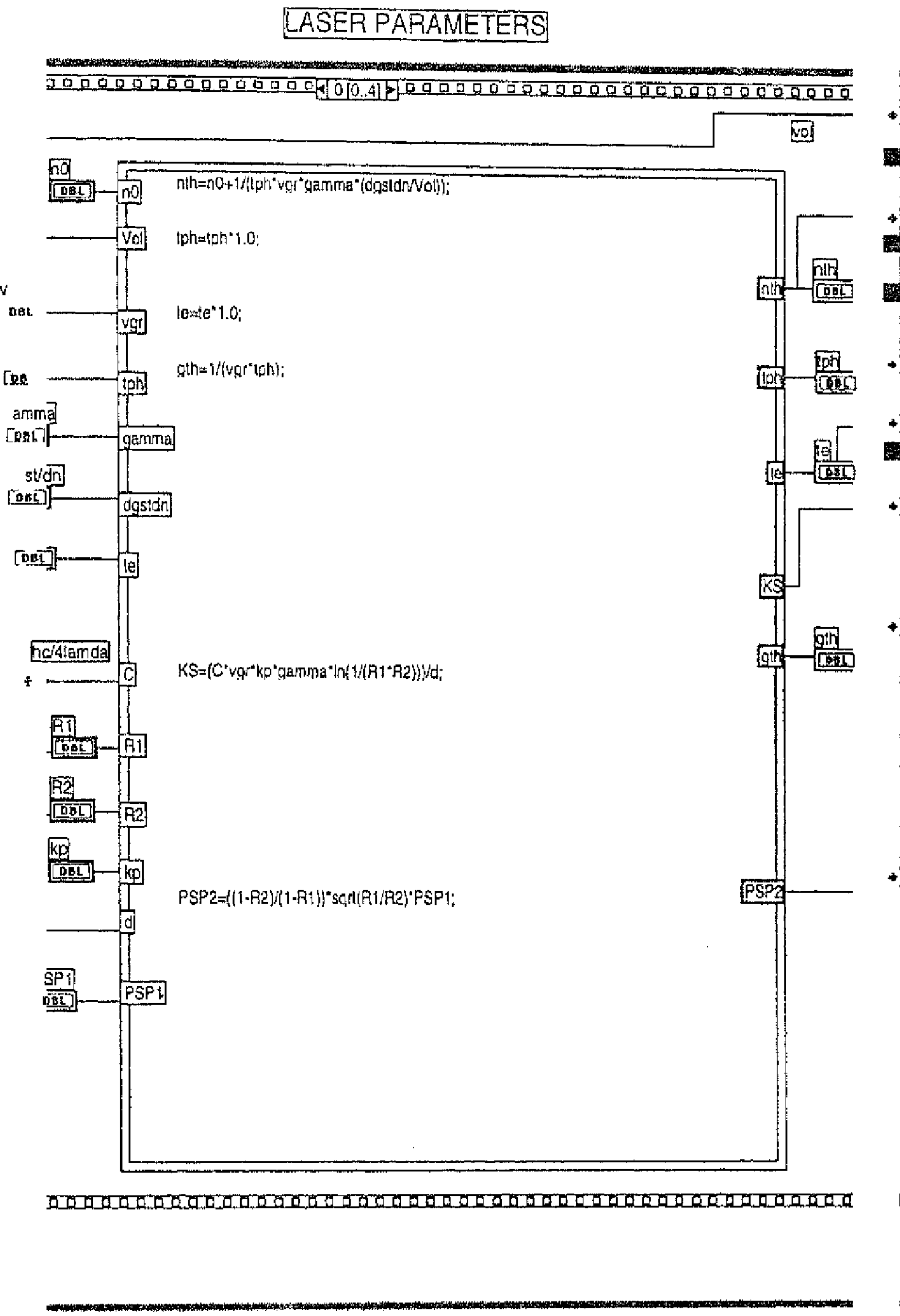

14 27

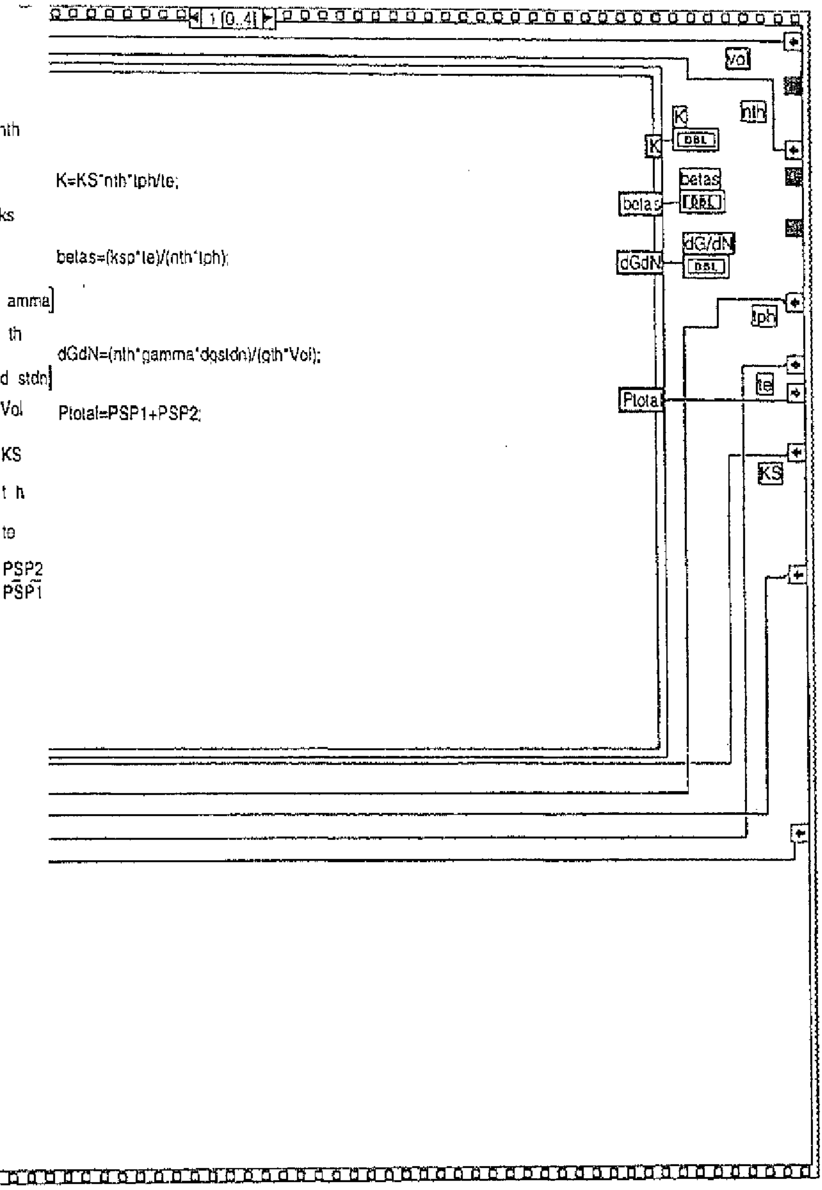
1 [0..4]
nth
K=KS*nth*tph/te;
ks
betas=(ksp*te)/(nth*tph);
amma
th
dGdN=(nth*gamma*dgstdn)/(gth*Vol);
d stdn
Vol
Ptotal=PSP1+PSP2;
KS
t h
te
PSP2
PSP1
Vol
nth
K
DBL
betas
DBL
dG/dN
DBL
K
betas
dGdN
tph
te
Ptotal
KS

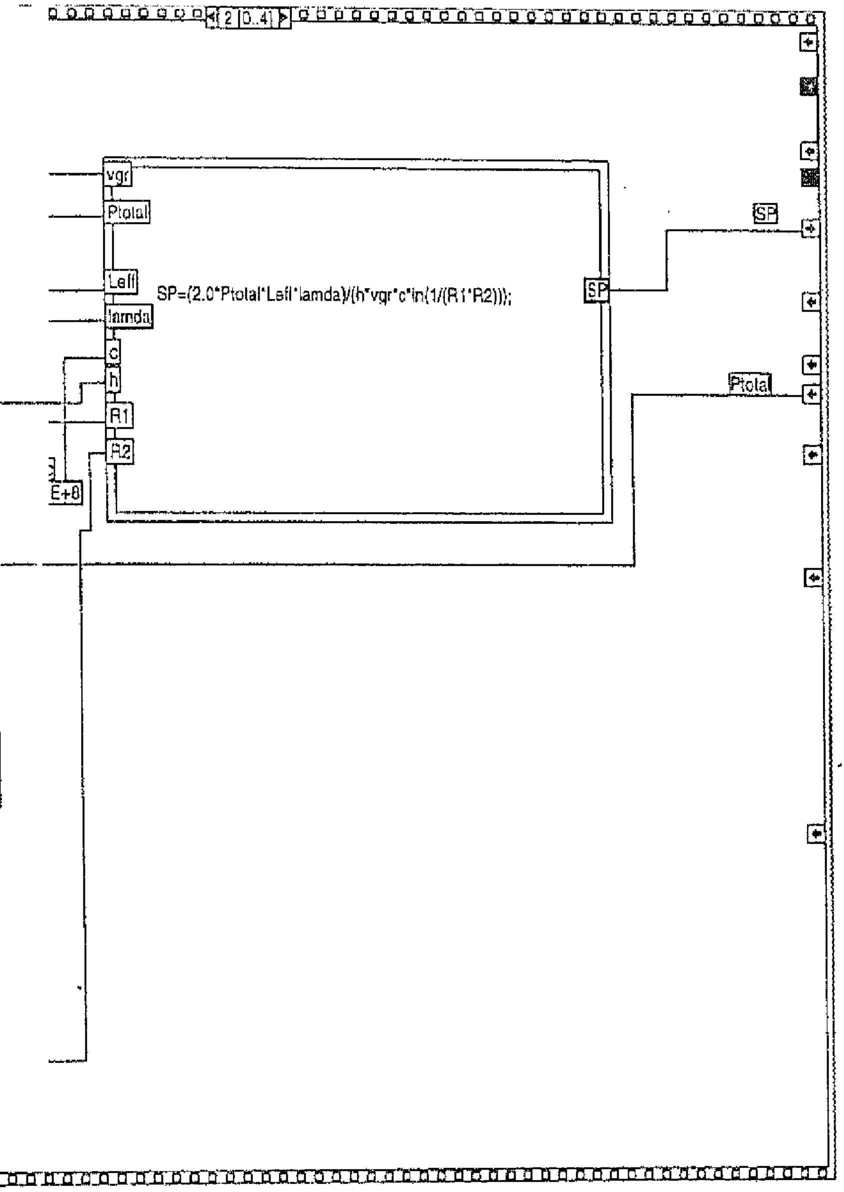
2 [0..4]
vgr
Ptotal
Leff
lamda
c
h
R1
R2
E+8
SP=(2.0*Ptotal*Leff*lamda)/(h*vgr*c*ln(1/(R1*R2)));
SP
SP
Ptotal

rameter v
ast moa f ed on 07 12 98 at 14 27
inted on 15.12.98 at 18:31

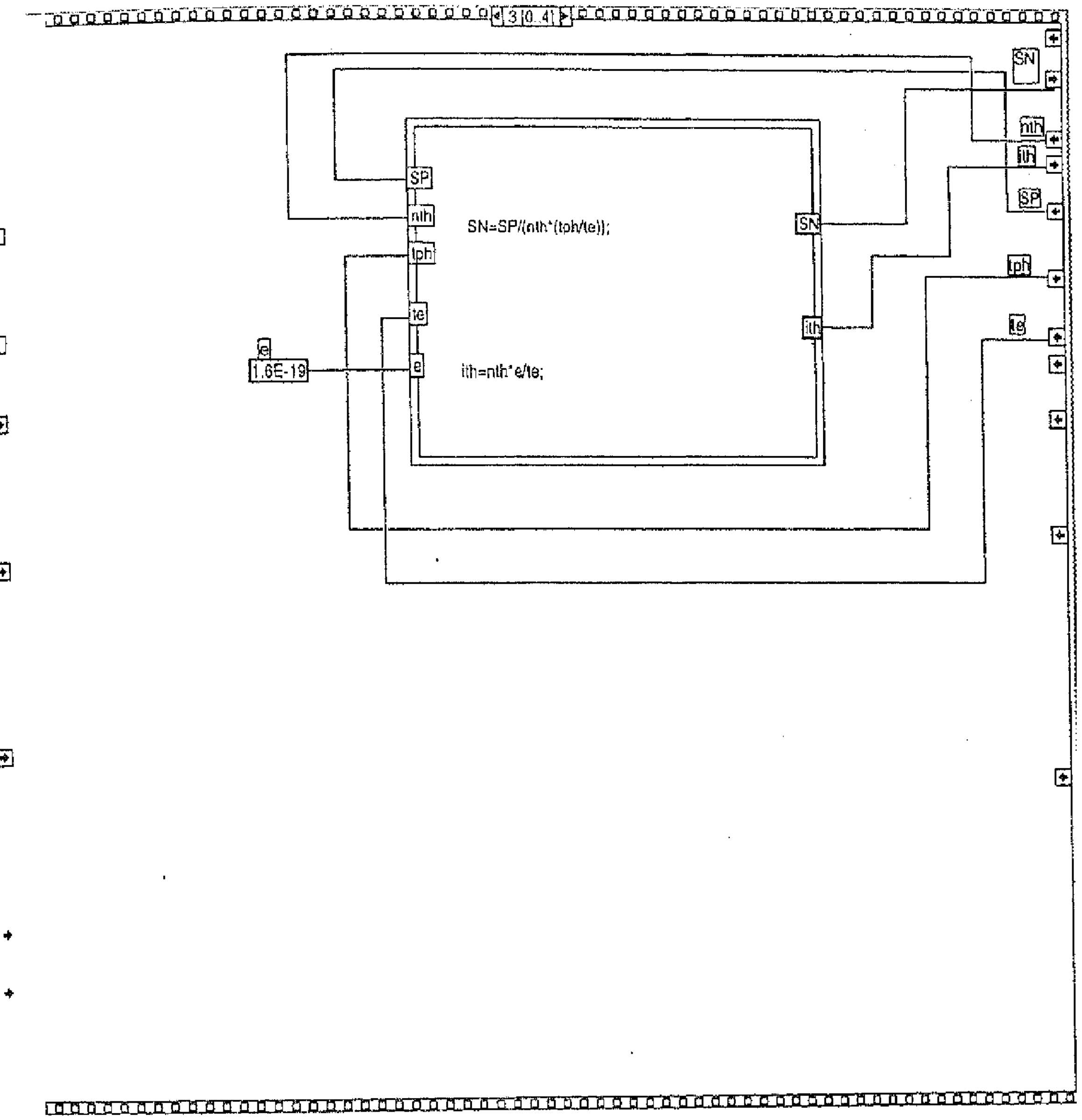

P

t 14 27

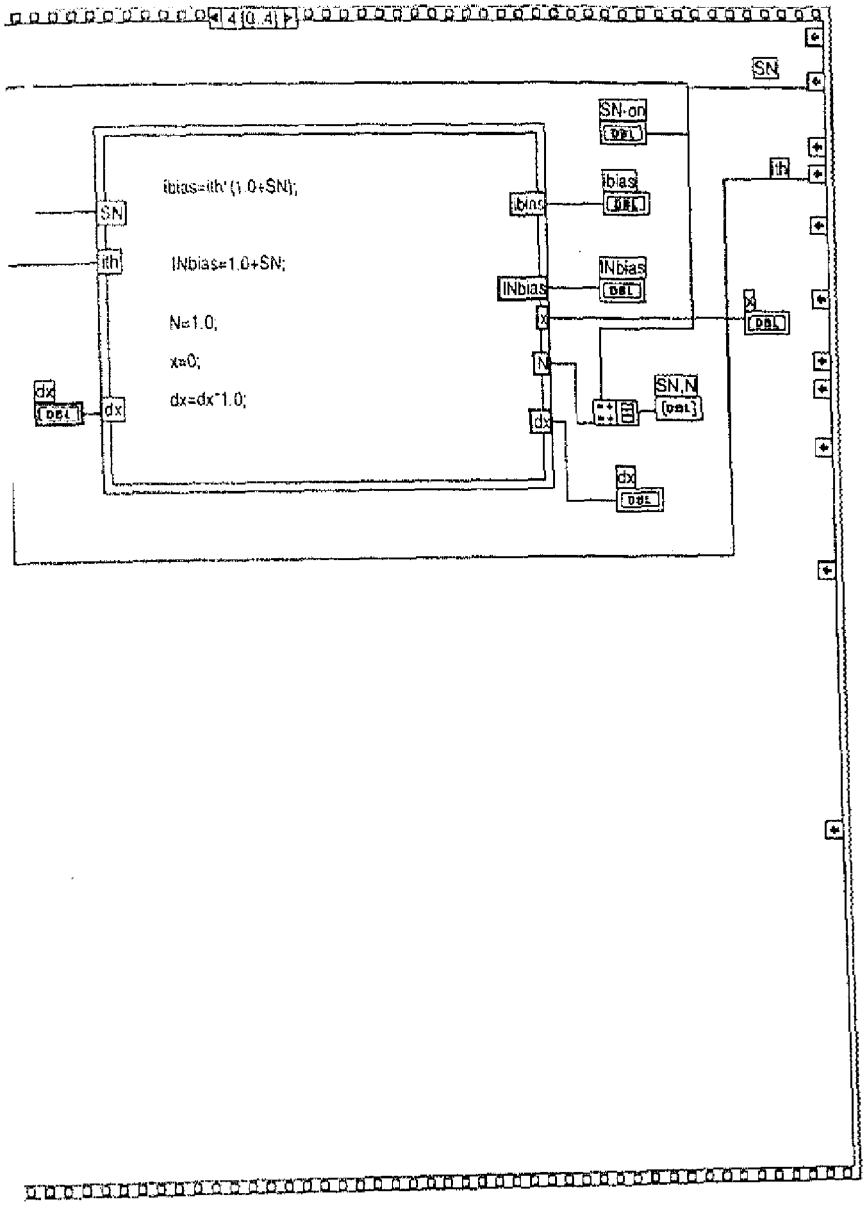

4 [0..4]
SN
SN-on
ith
ibias=ith*(1.0+SN);
INbias=1.0+SN;
N=1.0;
x=0;
dx=dx*1.0;
SN
ith
dx
ibias
INbias
x
N
dx
ibias
INbias
x
SN,N
dx
DBL

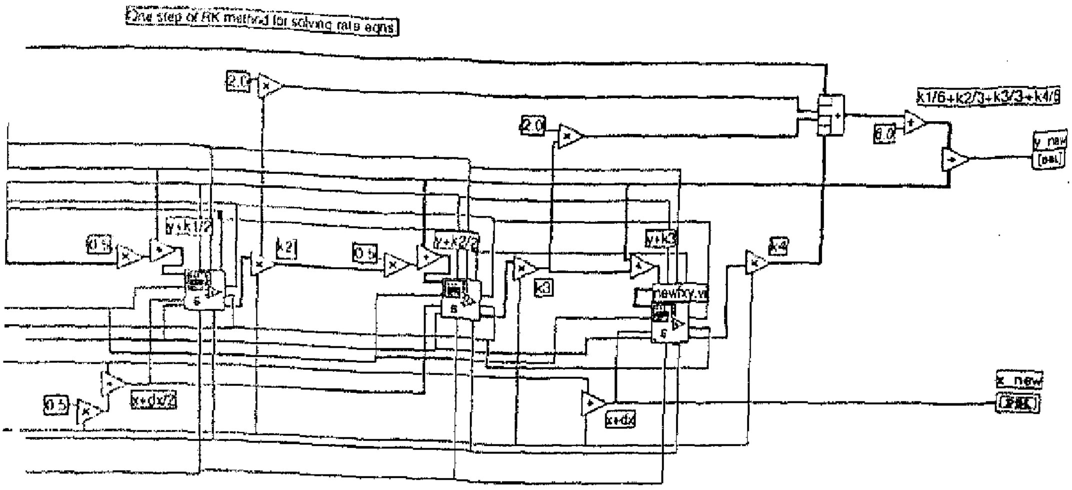
One step of RK method for solving rate eqns
2.0
2.0
k1/6+k2/3+k3/3+k4/6
6.0
y_new
0.5
y+k1/2
k2
0.5
y+k2/2
k3
y+k3
newfxy.vi
k4
0.5
x+dx/2
x+dx
x_new

newfxy v
Last mod f ed on 04 12 98 at 4 36
Printed on 15.12.98 at 18:38

Block Diagram

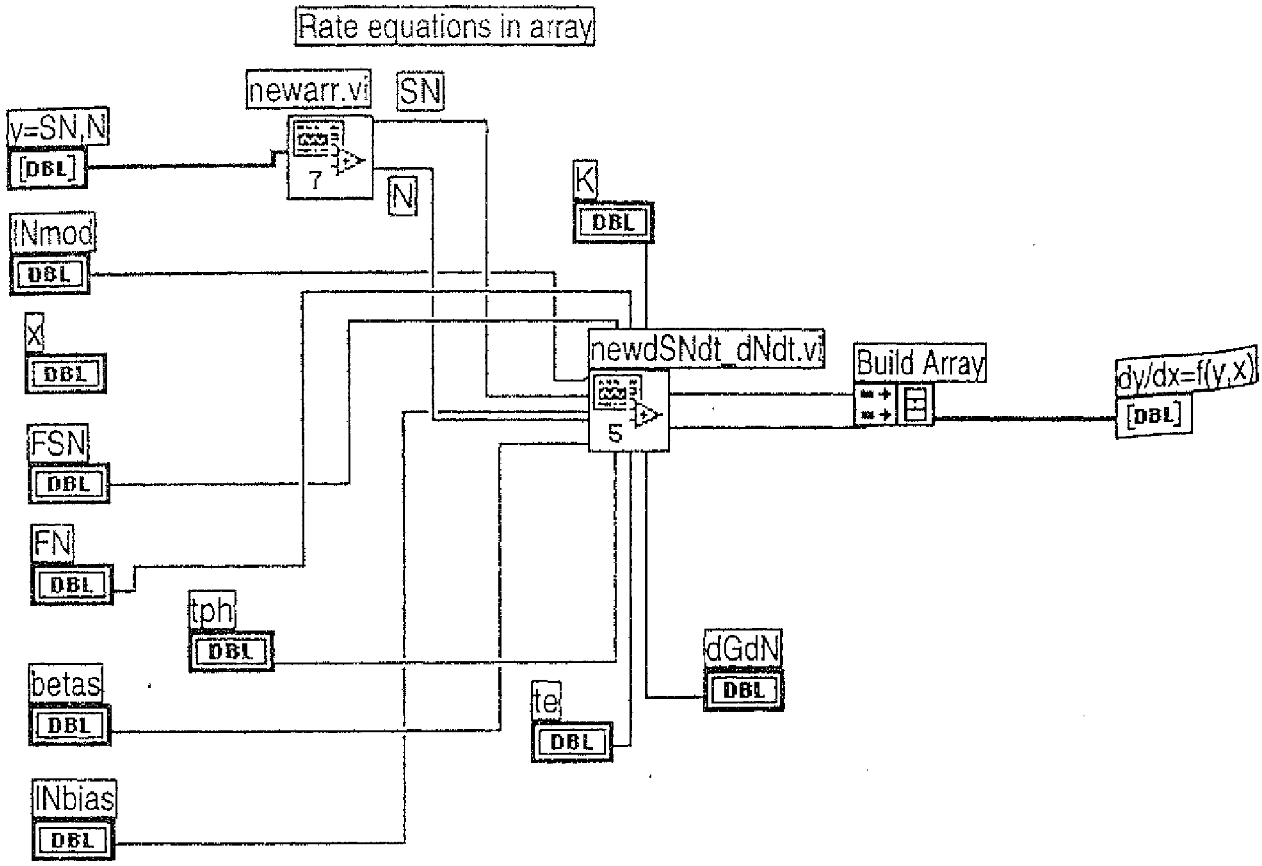

4 12 98 at 4 5
8 at 18:39

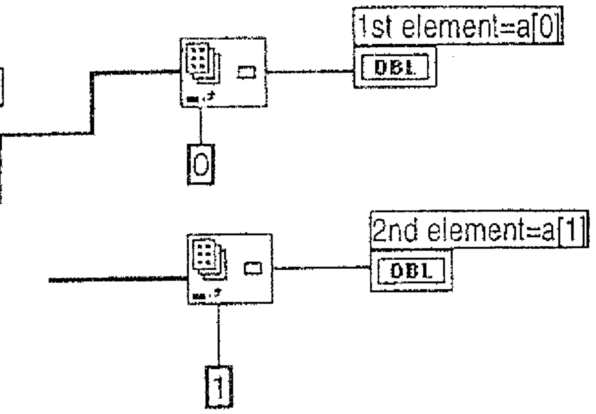

2 98 at 14 45
t 18:39

Normalised photon & electron rate equations

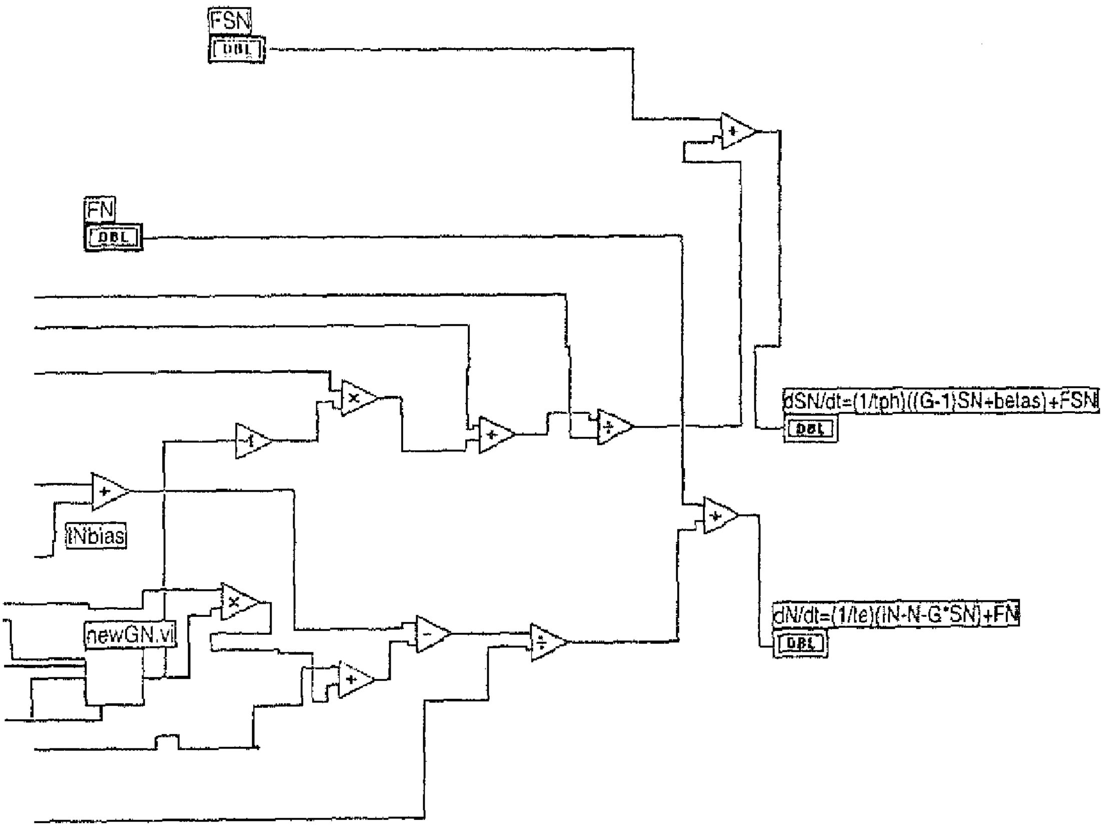

newGN v
Last mod f ed on 04 12 98 at 14 48
Printed on 15.12.98 at 18:39

Block Diagram

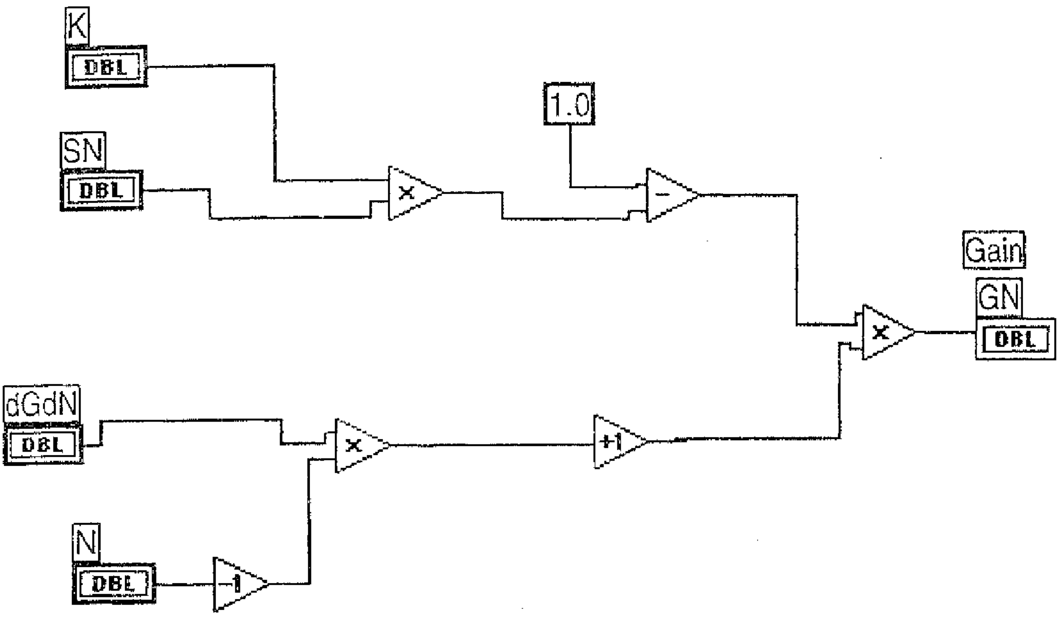

no VI
Last modified on 27.11.98 at 15:26
Printed on 15.12.98 at 18:40

Page 1

Fsn
FN

Block Diagram

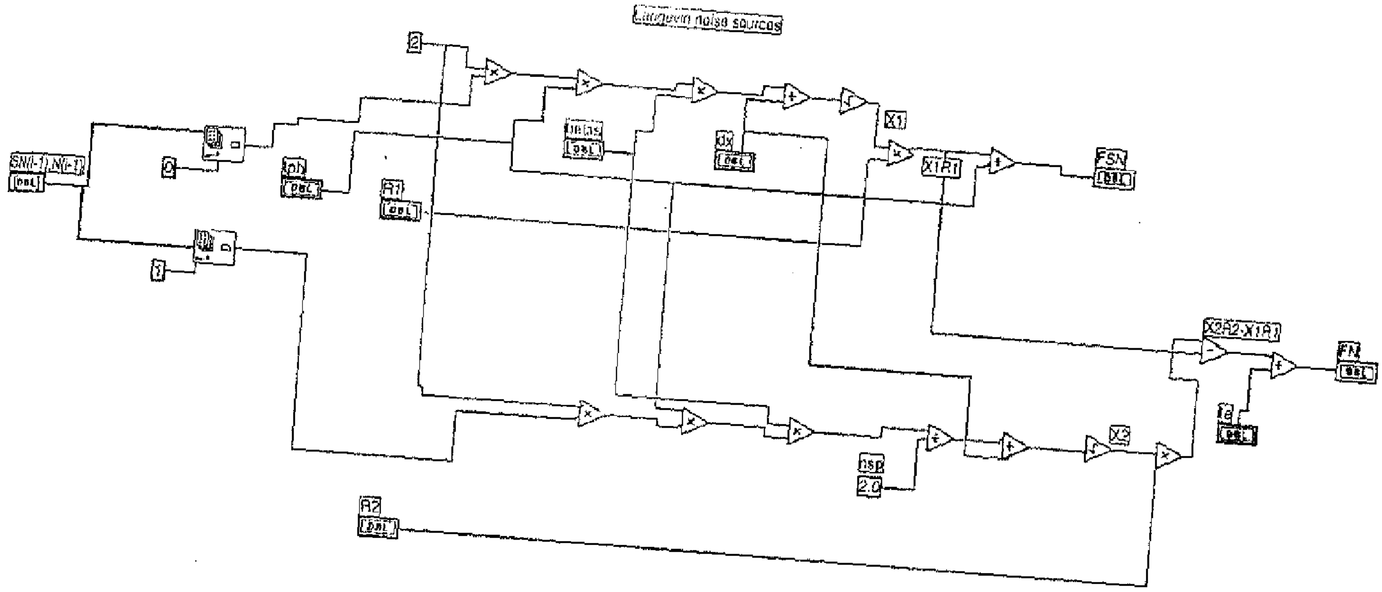

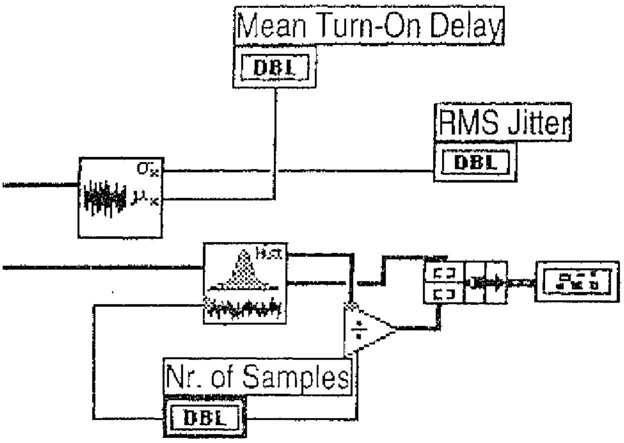
Mean Turn-On Delay
DBL
RMS Jitter
DBL
Nr. of Samples
DBL

? 98 at 12:17
14:59

tp

50E-12	3.60E-12	3.70E-12	3.80E-12	3.90E-12	4.00E-12	4.10E-12	4.20E-12	4.30E-12
8 21E+7	8.10E+7	7.99E+7	7.88E+7	7.78E+7	7.68E+7	7.59E+7	7.49E+7	7.41E+7
49E+7	7.39E+7	7.29E+7	7.19E+7	7.10E+7	7.01E+7	6.92E+7	6.84E+7	6.76E+7
6 94E+7	6.84E+7	6.75E+7	6.66E+7	6.57E+7	6.49E+7	6.41E+7	6.33E+7	6.26E+7
49E+7	6.40E+7	6.31E+7	6.23E+7	6.15E+7	6.07E+7	6.00E+7	5.93E+7	5.86E+7
12E+7	6.03E+7	5.95E+7	5.87E+7	5.80E+7	5.72E+7	5.65E+7	5.59E+7	5.52E+7
5 81E+7	5.72E+7	5.65E+7	5.57E+7	5.50E+7	5.43E+7	5.36E+7	5.30E+7	5.24E+7
5 54E+7	5.46E+7	5.38E+7	5.31E+7	5.24E+7	5.18E+7	5.11E+7	5.05E+7	4.99E+7
30E+7	5.23E+7	5.15E+7	5.09E+7	5.02E+7	4.96E+7	4.90E+7	4.84E+7	4.78E+7
09E+7	5.02E+7	4.95E+7	4.89E+7	4.82E+7	4.76E+7	4.70E+7	4.65E+7	4.59E+7
4 91E+7	4.84E+7	4.77E+7	4.71E+7	4.65E+7	4.59E+7	4.53E+7	4.48E+7	4.43E+7
4 74E+7	4.67E+7	4.61E+7	4.55E+7	4.49E+7	4.43E+7	4.38E+7	4.33E+7	4.28E+7
4 59E+7	4.53E+7	4.46E+7	4.40E+7	4.35E+7	4.29E+7	4.24E+7	4.19E+7	4.14E+7
4 45E+7	4.30E+7	4.33E+7	4.27E+7	4.22E+7	4.17E+7	4.11E+7	4.06E+7	4.02E+7
33E+7	4.27E+7	4.21E+7	4.16E+7	4.10E+7	4.05E+7	4.00E+7	3.95E+7	3.90E+7
4 21E+7	4.15E+7	4.10E+7	4.04E+7	3.99E+7	3.94E+7	3.89E+7	3.84E+7	3.80E+7
4 11E+7	4.05E+7	3.99E+7	3.94E+7	3.89E+7	3.84E+7	3.79E+7	3.75E+7	3.70E+7
4 01E+7	3.95E+7	3.90E+7	3.84E+7	3.80E+7	3.75E+7	3.70E+7	3.66E+7	3.61E+7
91E+7	3.86E+7	3.81E+7	3.76E+7	3.71E+7	3.66E+7	3.62E+7	3.57E+7	3.53E+7
83E+7	3.77E+7	3.72E+7	3.67E+7	3.63E+7	3.58E+7	3.54E+7	3.49E+7	3.45E+7
0 00E+0	0.00E+0	0.00E+0	0.00E+0	0.00E+0	0.00E+0	0.00E+0	0.00E+0	0.00E+0
0 00E+0	0.00E+0	0.00E+0	0.00E+0	0.00E+0	0.00E+0	0.00E+0	0.00E+0	0.00E+0
0 00E+0	0.00E+0	0.00E+0	0.00E+0	0.00E+0	0.00E+0	0.00E+0	0.00E+0	0.00E+0
0 00E+0	0.00E+0	0.00E+0	0.00E+0	0.00E+0	0.00E+0	0.00E+0	0.00E+0	0.00E+0
0 0E+0	0.00E+0	0.00E+0	0.00E+0	0.00E+0	0.00E+0	0.00E+0	0.00E+0	0.00E+0

98 at 12:17
14:58

ram for matching the experimental values of relaxation resonance freq.(fr),threshold current(ith) and laser characteristics